Accepted Manuscript

Geological Society, London, Special Publications

Glacial seismic geomorphology and Plio-Pleistocene ice sheet history offshore northwest Europe

Andrew M. W. Newton, Aleksandr Montelli, Christine L. Batchelor, Benjamin Bellwald, Rachel Harding, Mads Huuse, Julian A. Dowdeswell, Dag Ottesen, Ståle E. Johansen & Sverre Planke

DOI: https://doi.org/10.1144/SP525-2023-117

To access the most recent version of this article, please click the DOI URL in the line above. When citing this article please include the above DOI.

Received 19 June 2023
Revised 10 November 2023
Accepted 16 November 2023

Glacial seismic geomorphology and Plio-Pleistocene ice sheet history offshore northwest Europe

Andrew M. W. Newton[1*], Aleksandr Montelli[2], Christine L. Batchelor[3], Benjamin Bellwald[4,5], Rachel Harding[6], Mads Huuse[7], Julian A. Dowdeswell[2], Dag Ottesen[8], Ståle E. Johansen[9], Sverre Planke[5,10]

[1]School of Natural and Built Environment, Queen's University Belfast, University Road, Belfast, BT7 1NN, UK

[2]Scott Polar Research Institute, University of Cambridge, Cambridge, CB2 1ER, UK

[3]School of Geography, Politics and Sociology, Newcastle University, Newcastle Upon Tyne, NE1 7RU, UK

[4]Norwegian Geotechnical Institute (NGI), Sandakerveien 140, N-0484 Oslo, Norway

[5]Volcanic Basin Petroleum Research (VBPR) AS, Oslo Science Park, Gaustadalléen 21, N-0349 Oslo, Norway

[6]School of Archaeological and Forensic Sciences, University of Bradford, Bradford, BD7 1DP, UK

[7]Department of Earth and Environmental Sciences, University of Manchester, Oxford Road, Manchester, M13 9PL, UK

[8]Geological Survey of Norway, N-7040, Trondheim, Norway

[9]Center for Geophysical, Norwegian University of Science and Technology, Trondheim N-7031, Norway

[10]Centre for Earth Evolution and Dynamics (CEED), University of Oslo, Norway

* Correspondence to A.M.W. Newton (amwnewton@gmail.com)

Abstract

Plio-Pleistocene records of ice-rafted detritus suggest northwest European ice sheets regularly reached coastlines. However, these records provide limited insight on the frequency, extent, and dynamics of ice sheets delivering the detritus. Three-dimensional reflection seismic data of the northwest European glaciated margin have previously documented buried landforms that inform us on these uncertainties. This paper reviews and combines these existing records with new seismic geomorphological observations to catalogue landform occurrence along the European glaciated margin and considers how they relate to ice sheet history. The compilation shows Early Pleistocene ice sheets regularly advanced across the continental shelves. Early Pleistocene sea level reconstructions demonstrate lower magnitude fluctuations compared to the Middle-Late Pleistocene, and more extensive/frequent Early Pleistocene glaciation provides a possible mismatch with sea level reconstructions. This evidence is discussed with global records of glaciation to consider possible impacts on our wider understanding of Plio-Pleistocene climate changes, in particular how well Early Pleistocene sea level records capture ice sheet volume changes. Resolving such issues relies on how well landforms are dated, whether they can be correlated with other proxy datasets, and how accurately these proxies reconstruct the magnitudes of past climatic changes. Many questions about Pleistocene glaciation in Europe and elsewhere remain.

1. Introduction

The mid-Neogene opening of the Fram Strait contributed to enhanced deep-water exchange in the Nordic Seas and a gradual cooling of the Northern Hemisphere climate. This is evidenced by the first appearance of ice-rafted debris (IRD) from the northern Barents Sea region in the Fram Strait at ~14 Ma (Knies and Gaina 2008). Further south on the Vøring Plateau, IRD has been observed sporadically from ~12 Ma (Fig. 1), though the provenance of the material is uncertain (Mangerud *et al.* 1996). From ~2.8 Ma the persistence and volume of IRD observed in the Nordic Seas increases as Northern Hemisphere ice sheet development becomes more synchronous (Jansen and Sjøholm 1991; Kleiven *et al.* 2002). This was accompanied by changes in global atmospheric and oceanic circulation patterns (Hayashi *et al.* 2020; Bridges *et al.* 2023; McClymont *et al.* 2023) as the Earth transitioned to more extreme glacial-interglacial cycles (Lisiecki and Raymo 2005), with ice sheets now capable of reaching lower latitudes (e.g., Balco *et al.* 2005; Rea *et al.* 2018).

The ~2.8 Ma intensification of glaciation meant that the regular advance of ice sheets across palaeo-coastlines provided a major control on the sedimentary evolution of mid- and high-latitude continental margins (Holtedahl 1967; Rea *et al.* 2018; Batchelor *et al.* 2019; Montelli *et al.* 2019). While the global oxygen isotope record provides information on the volume of these ice sheets (Lisiecki and Raymo 2005), and the provenance of IRD can yield knowledge on where they reached coastlines (Jansen and Sjøholm 1991; Jansen *et al.* 2000), information on the configuration of palaeo-ice sheets requires additional methods. This includes exploring landform and sediment assemblages left behind by palaeo-ice sheets that have been, at least partially, preserved in the glacigenic sedimentary succession offshore (Dowdeswell *et al.* 2007, 2016).

Three-dimensional (3D) reflection seismic images have revolutionised our understanding of sedimentary basins globally, including a range of glaciated margins where the imaging of partially-preserved palaeo-seafloor surfaces has shown glacial landforms. Recent studies from northwest Europe have used basin-scale reflection seismic datasets to document buried glacial landforms and reconstruct past environmental changes and processes through the late Pliocene and Pleistocene (Montelli *et al.* 2017, 2018a; Newton *et al.* 2018; Rea *et al.* 2018; Bellwald *et al.* 2023). In this paper, existing evidence of buried glacial landforms on the northwest European margin are reviewed and combined with new observations from a ~180,000 km^2 3D reflection seismic database. The seismic geomorphological evidence of glacial landforms are catalogued for their spatio-temporal variability and discussed with sedimentary records from the North, Norwegian, and Barents Seas to explore what these observations mean for reconstructing the Plio-Pleistocene ice sheet history of northwest Europe. A key objective of this work was to bring together the somewhat disparate knowledge from different parts of the margin and to consider this evidence from a global perspective of Plio-Pleistocene climate change, with an emphasis on the potential implications of an apparent mismatch between global ice sheet histories and concomitant sea level changes.

2. Geological background

2.1 Shelf morphology

The study area encompasses a latitudinal transect from the southern North Sea to the Bjørnøyrenna Trough Mouth Fan in the southwestern Barents Sea, i.e. between 52-74 °N (Fig. 1). Bathymetry shows the contemporary morphology of the continental shelf is largely characterised by shallow banks (100-200 m depth) and cross-shelf troughs (300-500 m depth) that terminate at the shelf edge (Fig. 1). The troughs represent the flow pathways of ice streams during the last glacial cycle (Ottesen *et al.* 2005a, b; Rydningen *et al.* 2013; Montelli *et al.* 2017; Newton and Huuse 2017b). The evolution of the North Sea is also impacted by glaciation, but, with the exception of the Norwegian Channel (up to ~700 m depth) (Sejrup *et al.* 2003), the bathymetry is typically less than ~200 m deep and the surface geomorphology records evidence for extensive meltwater networks and large moraine complexes from the most recent glaciations (Bradwell *et al.* 2008). Continental shelf width along the margin varies from the large epicontinental shelves of the Barents and North Seas, to the 50-200 km-wide shelf along the mid-Norwegian margin (Fig. 1). At its narrowest, the shelf is ~30 km offshore Troms in northern Norway, where the shelf edge is heavily canyonised (L'Heureux *et al.* 2013). Shelf edge water depths are typically 300-400 m (up to 500 m in cross-shelf troughs). The continental slope dip varies along the margin, dipping by ~1 ° on the mid-Norwegian margin to as much as 3-5 ° to the Lofoten and Møre Basins. In areas along the margin impacted by Middle-Late Pleistocene slope failure, the headwall scarps can dip by up to ~30 ° (Nielsen *et al.* 2005). Water depths increase downslope to 1000-1500 m on the Vøring Plateau and up to 3000 m in the adjacent abyssal plains of the Lofoten and Møre basins.

2.2. Stratigraphic schemes of the northwest European margin

In the southwest Barents Sea, the up to ~3.5 km-thick glacial stratigraphy is divided into three seismic units separated by regional seismic reflections (GI, GII, and GIII) (Faleide *et al.* 1996; Andreassen and Winsborrow 2009; Alexandropoulou *et al.* 2021) (Fig. 2a). The oldest unit (GI) shows progradation driven by glacial sedimentary processes that began at ~2.7 Ma – based on increased IRD in well 7216/11-S – and lasted until ~1.5 Ma (Faleide *et al.* 1996; Dahlgren *et al.* 2005). Unit GII was deposited from ~1.5-0.7 Ma and is characterised on seismic profiles by chaotic reflections interpreted as slope debrites and megaslides (Hjelstuen *et al.* 2007), with palaeo-shelf deposits reflecting deposition by grounded glaciers. The youngest Unit (GIII) was deposited from 0.7 Ma and is comprised of stacked chaotic seismic reflections interpreted as glacigenic debris flows on the slope (Hjelstuen *et al.* 2007). Shelf deposits are similar to those from Unit GII. A key characteristic of the Barents Sea glacigenic stratigraphy is the presence of a major upper regional unconformity (BS-URU) (Faleide *et al.* 1996). This is a composite surface that can be correlated across much of the Barents Sea and was formed in response to repeated ice sheet erosion of sedimentary bedrock.

The northern Norwegian margin glacial stratigraphy offshore Troms (Fig. 1) is up to ~1.2 km thick, can be correlated with the southwest Barents Sea and the mid-Norwegian Naust Formation, and is divided into three main seismic units bounded by unconformities and seismic facies changes (Rydningen *et al.* 2016) (Fig. 2b). Seismic Unit S2 marks the onset of glacial progradation from ~2.7 Ma and consists of low-angle clinoforms that transition into the high-angle clinoforms of Unit S3 from ~1.5 Ma (Rydningen *et al.* 2016). The youngest unit (S4) is characterised by aggradational seismic geometries and has two hypothesised ages for its onset (0.2 Ma or 0.7 Ma). The base of this uppermost unit is bounded by an unconformity (T-URU) analogous to the BS-URU to the north and an unconformity on the mid-Norwegian margin to the south.

Offshore mid-Norway, the late Plio-Pleistocene Naust Formation is up to ~1 km thick and largely comprised of low-angle sediment wedges and up to 150 km of progradation (Dahlgren *et al.* 2002a; Ottesen *et al.* 2009; Rise *et al.* 2010) (Fig. 2c). Some deposits continue down-dip of Cenozoic inversion structures as thin, acoustically-stratified deposits that comprise some of the continental slope. Fine-grained diamicts with angular gravels and sandy layers have been observed in core (Dahlgren *et al.* 2002a; Ottesen *et al.* 2009). The Naust Formation has been divided into five main depositional sequences – N (2.8-1.5 Ma), A (1.5-0.8 Ma), U (0.8-0.4 Ma), S (0.4-0.2 Ma), and T (0.2-0 Ma) – with the onset of deposition related to a spike in IRD at ~2.8 Ma (Jansen and Sjøholm 1991; Eidvin *et al.* 2000; Jansen *et al.* 2000; Ottesen *et al.* 2012). The mid-Norwegian margin has a prominent upper regional unconformity (MN-URU) associated with time-transgressive glacial erosion that typically marks the base of Naust T (Dahlgren *et al.* 2005; Rise *et al.* 2005).

Although complicated by the narrow shelf to the north, the onset of glacigenic deposition in the northern North Sea can be correlated with the base of the Naust Formation on the mid-Norwegian margin and core evidence showing silty/sandy diamicts (wells 34/7-1, 34/4-7, and 34/8-1) (Fig. 1) (Eidvin *et al.* 1998, 2000; Ottesen *et al.* 2009; Batchelor *et al.* 2017). The up to 1.6 km-thick glacial stratigraphy has been divided into four units (Ottesen *et al.* 2014, 2018; Batchelor *et al.* 2017; Løseth *et al.* 2022) (Fig 2d). Units A and B are comprised of acoustically semi-transparent deposits and demonstrate westerly progradation (Løseth *et al.* 2020, 2022). Coeval with Units A and B, deposition of a shelf edge delta on the East Shetland Platform meant the basin was being infilled from different directions (Ottesen *et al.* 2014; Lloyd *et al.* 2021a). Unit C consists of geometries similar to Units A and B, but with increased observations of lobate deposits (Batchelor *et al.* 2017). Collectively, progradation of Units A to C complete the infill of the northern North Sea basin before Unit D then marks northward progradation towards the Møre Basin (Batchelor *et al.* 2017). This unit includes the Middle and Late Pleistocene sediments of the North Sea Fan (Sejrup *et al.* 2000; Rise *et al.* 2004; Nygård *et al.* 2005). Similar to elsewhere, the northern North Sea has a prominent Upper Regional Unconformity (NS-URU) (~0.8-0.5 Ma) that extends across most of the eastern North Sea and can be partially mapped into the central North Sea (Ottesen *et al.* 2018).

While the sedimentary depocentre of the northern North Sea does not continue into the central and southern North Sea, the top bounding surface of Unit B and the NS-URU equivalent (a surface equivalent to the NS-URU, that is not necessarily an unconformity) can be traced into the central basin of the North Sea (Ottesen *et al.* 2018). In the central and southern North Sea the Pleistocene stratigraphy measures up to 1.2 km thick (Lamb *et al.* 2018; Rea *et al.* 2018) and numerous seismic stratigraphic schemes have been developed (Fig. 2e-g). Here, the compilation by Ottesen *et al*. (2018) is preferred because it is spatially-extensive and correlates several stratigraphic regimes. The evolution of the southern and central North Sea through the Pleistocene are closely linked and described chronologically.

At the Pleistocene onset, infill of the basin began in the Dutch sector of the southern North Sea (Nielsen *et al.* 2007; Thöle *et al.* 2014). Tying of borehole A15-03 to 3D seismic data has allowed extension of biostratigraphic and palaeomagnetic constraints across the basin, meaning it is the best dated part of the entire margin (Kuhlmann and Wong 2008; Harding 2015; Lamb *et al.* 2018; Ottesen *et al.* 2018). As the southernmost part of the North Sea was infilled by fluvio-deltaic sediments (Units 5-13 – Fig. 2g), westward progradation occurred until ~2.35 Ma when it switched to north-westward (Kuhlmann and Wong 2008; Lamb *et al.* 2018). Accommodation in the southern North Sea was largely infilled by ~1.8 Ma, meaning that Early-Middle Pleistocene units of the central and northern North Sea are not present in appreciable thicknesses across the southern North Sea (Kuhlmann and Wong 2008; Lamb *et al.* 2018; Ottesen *et al.* 2018). Instead, above this, the southern North Sea stratigraphic nomenclature is more piecemeal and spatially-limited due an extensive time-transgressive unconformity (Moreau *et al.* 2012; Phillips *et al.* 2017; Benvenuti *et al.* 2018).

Clinoform Units 2 and 3 are comprised of prograding sediment wedges and were deposited after the southern North Sea was infilled, with most sediment coming from the east and southeast (Lamb *et al.* 2018; Ottesen *et al.* 2018). As Clinoform Units 1-3 were being deposited, Unit Z was deposited on the British side of the central North Sea (Ottesen *et al.* 2014) (Fig. 2e). Its upper, irregular surface is broadly coeval with the top of Clinoform Unit 3, and its base with the start of the Pleistocene (Rundberg and Eidvin 2005; Ottesen *et al.* 2014). After deposition of Clinoform Units 1-3 and Unit Z, the Central Basin Unit was deposited in the latter part of the Early Pleistocene (Ottesen *et al.* 2014). The top of the Central Basin Unit is interpreted as the NS-URU equivalent and merges with an unconformity in the southern North Sea (Moreau *et al.* 2012; Ottesen *et al.* 2018). Sediments above the NS-URU equivalent provide the final removal of accommodation in the central North Sea (Ottesen *et al.* 2014; Rea *et al.* 2018).

3. Data and methods

This study used a database of ~180,000 km^2 3D reflection seismic and basin-wide 2D seismic data on the northwest European margin. The database consists of several generations of data and vertical resolution is estimated to vary from ~10-40 m (based on frequencies ~30-60 Hz and P-wave velocity 1.8-2.2 km s^{-1}). While the coverage of 3D reflection seismic data is extensive, areas such as the Barents Sea and Troms are less well covered, meaning that the possible insights in these areas are more limited. In these areas, existing publications supplement the workflow.

The first stage of analysis was to use existing stratigraphic schemes (Fig. 2) and apply these to the available data. The main stratigraphic units do not assign a specific *a priori* control to their boundaries, but uses them to establish the geological framework in which seismic geomorphological interpretations can be placed. Once the various stratigraphic schemes were in place, the 3D seismic data were used to manually pick reflections as part of a standard seismic geomorphological workflow (Posamentier 2004; Posamentier *et al.* 2007, 2022). Criteria for picking reflections included those with strong/continuous reflection amplitudes and reflections which, when cut by times slices, contained evidence of glacial landforms. Key reflections were identified by investigating dip and strike seismic lines for evidence of glacigenic features. Picked reflections were studied as two-way-time surface maps under varied lighting conditions and seismic attributes – e.g., RMS amplitude and variance (Cox *et al.* 2020). The compilation of Dowdeswell *et al*. (2016) provides an extensive range of glacial landform analogues and was used to support interpretation of subsurface features.

Newly documented landforms were catalogued with those previously published (linked in the text with citations) and then combined to review landform occurrence. As robust geochronological constraints were unavailable, in order to ascribe tentative dates for individual surfaces, a basic assumption was applied that sedimentation rates were broadly linear between existing age constraints (Fig. 2), making suitable ad hoc allowances in the presence of strongly progradational architectures. Given the lack of dating constraints along the margin, this is an important caveat for any timeline reconstructions, so in order to minimise this as much as possible, we compare these relative dates with other better-dated proxy datasets (e.g., IRD) to determine potential coeval environmental changes and support reasonable age estimates. While several major submarine slides have impacted the glacial stratigraphy along the margin, and are associated with Pleistocene ice sheets and their sedimentation patterns, we do not focus on them here as they are not explicitly a glacial landform. A review of such features can be found in Newton and Huuse (2017b).

4. Glacial seismic geomorphology of Europe's glaciated margin

Seismic data offshore northwest Europe reveal a range of glacial landforms. In this section, new and previously documented examples (linked with citations) of glacial landforms are reviewed from palaeo-shelf/slope settings, to document the characteristics and abundance of different glacial landforms and their importance for environmental reconstruction (Table 1).

4.1. Subglacial landforms

4.1.1. Mega-scale glacial lineations

Along all parts of the margin streamlined features are observed on the seafloor within cross-shelf troughs (Newton and Huuse 2017b). These features have also been documented on buried palaeo-shelves and glacial unconformities (Fig. 3). They typically measure 100-300 m wide, tens of metres high, and several kilometres long – similar metrics to terrestrial landforms interpreted as mega-scale glacial lineations (MSGL) (Clark 1993; Spagnolo *et al.* 2014). MSGLs relate to the ploughing or accretion of subglacial sediments (Clark *et al.* 2003; King *et al.* 2009; Spagnolo *et al.* 2016) and are associated with fast-flowing ice, allowing reconstruction of palaeo-ice sheet configurations and sediment pathways (Ottesen *et al.* 2005a; Dowdeswell *et al.* 2006). In the Barents Sea, MSGL have been documented across large parts of the Bjørnøyrenna trough seafloor (Winsborrow *et al.* 2010), atop the buried BS-URU surface (Piasecka *et al.* 2016) (Fig. 3a), and buried on other Pleistocene surfaces within the three main stratigraphic units of the Bjørnøyrenna Trough Mouth Fan (Andreassen *et al.* 2004, 2007; Harishidayat *et al.* 2021). Similar features offshore Troms are found on the base of Unit S4 (a surface correlating with the BS-URU), and within a buried palaeo-trough (Rydningen *et al.* 2016). On the mid-Norwegian margin, multiple sets of MSGL have been previously observed (Montelli *et al.* 2017; Newton and Huuse 2017b), while some new examples, that are often only partly-preserved, are presented here and show that MSGL are present in all Naust units (Figs 2d and 3b-g). In the northern North Sea, MSGL are observed at the base of Unit D (Batchelor *et al.* 2017) (Figs 2d and 3h). In the central North Sea several generations of MSGL are observed in Clinoform Units 1, 2, and 3, with the earliest observed at ~1.87 Ma (Rea *et al.* 2018). Cores recovered through the interval preserving some of the earliest MSGL are predominantly characterised by subglacial and subaqueous glacial outwash fan sediments that represent a sequence of ice sheet advance, overriding, and retreat (Rea *et al.* 2018; Rose *et al.* 2018). In most cases along the margin, MSGL occur at the base of topographic lows that represent buried cross-shelf troughs. The repeated presence of MSGL, particularly on the mid-Norwegian margin show that their orientation varies between different sets (Fig. 3a, 3b, 3d, 3g), providing insights on ice stream pathway changes (e.g. Dowdeswell *et al.* 2006).

4.1.2. Hill-hole pairs and rafts

Hill-hole pairs are a tectonic feature formed when ice is frozen to the substrate and ice flow then displaces the substrate (Winsborrow *et al.* 2016; Bellwald *et al.* 2023). This typically results in the formation of a topographic depression followed downstream by a hill composed of the excavated material. On the contemporary seafloor, hill-hole pair features are observed in the Bjørnøyrenna cross-shelf trough and on the mid-Norwegian margin, where the surficial morphology generally consist of hills ~50-100 m above the surrounding seafloor and holes of a similar depth (Ottesen *et al.* 2005a; Rise *et al.* 2016; Winsborrow *et al.* 2016). Buried examples of hill-hole pairs and megablock rafts are uncommon, but both have been documented in the Barents Sea on the BS-URU surface (Andreassen *et al.* 2004; Bellwald *et al.* 2019, 2023) and hill-hole pairs have been observed on the mid-Norwegian margin within Naust T (Fig. 4b-4d). In each case their observation can be used to link ice flow with frozen bed conditions.

4.1.3. Crevasse-squeeze ridges

Networks of rhombohedral ridges on the seafloor have been observed across the Barents Sea (Newton and Huuse 2017a) and are interpreted as the injection of deformable materials into basal crevasses due to overburden pressures from the ice sheet (Evans and Rea 1999). These crevasse-squeeze ridges are left behind after the ice sheet down-wastes or it uncouples from the seafloor in marine settings due to increased buoyancy, providing evidence for ice stagnation. These features typically measure only a few metres in height, limiting both preservation potential and their ability to be imaged using reflection seismic data. As such, they have not been confidently documented in the subsurface anywhere on the margin except for new observations presented here on the base surface of Naust U (~800 ka) (Fig. 5b). Similar features have been observed upon the BS-URU in the Barents Sea, but these relate to the underlying polygonal fault network associated with possible collapse structures of pingos or thermokarst lakes (Bellwald *et al.* 2019) – highlighting the importance of understanding the equifinality of geomorphological processes.

4.1.4. Eskers and tunnel valleys

Meltwater landforms, typically eskers and tunnel valleys, can provide insights on past meltwater fluxes. Eskers are sinuous ridges of stratified materials that have been extensively observed onshore northwest Europe (Stroeven *et al.* 2016), but rarely offshore – e.g., in the central Barents Sea (Newton and Huuse 2017b) and the North Sea (Kirkham *et al.* 2021). Tunnel valleys are overdeepened valleys formed by meltwater beneath the ice sheet (Ó Cofaigh 1996) and are common in the North and Barents Seas. They can occur as anastomosing, dendritic, or isolated systems and are thought to form from steady state erosion or outburst meltwater floods (Huuse and Lykke-Andersen 2000b; Praeg 2003; Van Der Vegt *et al.* 2012; Kirkham *et al.* 2021).

In the central Barents Sea, numerous overdeepened erosional features on the seafloor have been interpreted as tunnel valleys. They are up to ~60 km long, 200-2500 m wide, 8-50 m deep, and relate to the last glacial cycle (Newton and Huuse 2017a). Similar features have been mapped eastward into the Kara Sea (Montelli *et al.* 2020). Offshore Troms there is currently no documentation of tunnel valleys, while only a few have been documented within the mid-Norwegian Naust Formation. Buried within Naust T on the northern part of the Trænadjupet cross-shelf trough, a new tunnel valley has been documented that is ~12 km long, ~400 m wide, and up to ~20 m deep (Fig. 6b). Further south, new tunnel valleys with similar dimensions are documented within Naust S and T (Fig. 6d-6e). In all three examples the valleys are highly sinuous with undulating thalwegs, suggesting that they were likely formed by pressurised meltwater on the mid-Norwegian margin.

In the North Sea, tunnel valleys are observed extensively, covering all parts of the northern, central and southern basins, except for the Norwegian Channel (Huuse and Lykke-Andersen 2000b; Moreau *et al.* 2012; Ottesen *et al.* 2020). Although geochronological constraints are limited, most tunnel valleys occur above the NS-URU and would have been formed during the last three major glaciations. Regional mapping in the northern and central North Sea has documented 2200 tunnel valleys, with their greatest density coeval with the areas of thickest sediment in the central North Sea (Ottesen *et al.* 2020). The tunnel valleys are typically less than 20 km long (but can measure up to ~150 km), 0.5-2 km wide, and 10s to 100s m deep (Ottesen *et al.* 2020). They have undulating thalwegs and variable orientations that are associated with changing subglacial drainage patterns. Multiple generations of tunnel valley formation are demonstrated by multi-cutting events on seismic profiles (Fig. 6g-6h). In the eastern and southern North Sea, and in adjacent onshore areas, tunnel valleys are equally prolific (Piotrowski 1994; Huuse and Lykke-Andersen 2000b; Kristensen *et al.* 2007; Moreau *et al.* 2012).

4.2. Ice-marginal landforms

4.2.1. Moraines and thrust structures

Linear and arcuate ridges, interpreted as moraines, are a common feature along the northwest European margin (Newton and Huuse 2017b) and are a useful indictor of past ice sheet extent and retreat patterns (Barr and Lovell 2014). On the contemporary seafloor, end moraines are observed along the entire margin in many fjords and on the continental shelf (Bradwell *et al.* 2008; Ottesen *et al.* 2008; Rydningen *et al.* 2013). Examples of buried moraines are uncommon due to a lack of preservation/imaging and examples are restricted to new observations presented here from within Naust units U, S, and T on the mid-Norwegian margin (Fig. 5a-5c). At the base of Naust U and S, multiple ridges 2-10 km long, 200-400 m wide, and up to 10 m high are observed on outer palaeo-shelves and are interpreted as retreat moraines. At the base of Naust T, an end moraine, measuring 14 km long, up to 2 km wide, and ~30 m high, with a chaotic and semi-transparent internal structure, represents a major stillstand event during retreat of the penultimate glacial cycle (Fig. 5d). Lateral shear margin moraines can be observed on the seafloor in a number of places along the margin as arcuate ridges up to 30 m high, ~4-8 km long, and ~1 km wide (Batchelor and Dowdeswell 2016; Ottesen *et al.* 2016b). They are typically adjacent to the cross-shelf troughs, with their long axis parallel to the trough. Buried along the margin they are less common than end moraines, but they have been observed in the Barents Sea above the BS-URU (Bellwald and Planke 2019). In the eastern and central North Sea, there is glacitectonic evidence in the form of folding, faulting, and dislocation of sediments (Fig. 4e, 4f). This includes buried thrust complexes related to gravity spreading in areas distal to the ice sheet margin and compressional forces proximal to it (Bendixen *et al.* 2018). This complex is not dated but the seismic stratigraphic framework suggests they could be Marine Isotope Stage (MIS) 16. Similar structures are observed in the eastern North Sea, where ice sheet advance has caused up to 200 m of horizontal displacement on individual thrusts (Huuse and Lykke-Andersen 2000a). In the southwest Barents Sea, reflection seismic capture similar deformation structures of Cretaceous bedrock below the BS-URU (Bellwald *et al.* 2019).

4.2.2. Grounding-zone wedges and outwash fans

Asymmetric wedges with chaotic and laminated internal stratigraphy, that are typically several kilometres in length, the width of any constraining topography, and a height generally of a few tens of metres, have been interpreted as grounding-zone wedges (GZWs) (Dowdeswell *et al.* 2008;

Batchelor and Dowdeswell 2015). Subaqueous outwash fans show similar seismic geometries and are associated with point sources of meltwater. These landforms provide insights on ice flow directions, grounding line and meltwater locations, and retreat dynamics of former ice masses (Dowdeswell *et al.* 2008). GZWs have been observed on the contemporary seafloor in most cross-shelf troughs along the margin and are dated, or are assumed to date, to the last glacial cycle (Ottesen *et al.* 2005a, 2016a; Laberg *et al.* 2009; Winsborrow *et al.* 2010; Rydningen *et al.* 2013; Sejrup *et al.* 2016; Newton and Huuse 2017a). Seismic records have identified a limited number of buried GZWs on the mid-Norwegian margin (Dahlgren *et al.* 2002b; Montelli *et al.* 2017), with an additional example within Naust U documented here (Fig. 5e). In the Norwegian Channel, a c. 30-meter thick sandy deposit above the NS-URU, with low seismic velocities and low density values, contains the Peon gas discovery and has been interpreted as an ice-marginal outwash fan, sealed by high-velocity and high-density glacigenic sediments (Bellwald *et al.* 2022) (Fig. 5f-5g). The overall lack of buried fan-like features, compared with their regular presence on the contemporary seafloor, may relate to difficulties in seismic imaging or from glacial reworking of landforms during ice sheet advance causing reworking of the upper strata of a GZW, forming “till tongues” (King 1993). The subsequent creation of sheet-like seismic geometries are ambiguous to interpret because key characteristics, such as the asymmetric and positive relief geometry of the GZW, may be more difficult to discern – making it harder to differentiate whether strata reflect subglacial till emplacement or ice-marginal deposition.

4.3. Proglacial landforms

4.3.1. Iceberg scours

Iceberg scours (or ploughmarks) are the most common feature observed on glaciated margins. They are usually u- or v-shaped and linear or curvilinear erosional features that form when an iceberg keel makes contact with the seabed and disturbs the seafloor as the iceberg is moved by ocean currents (Woodworth-Lynas *et al.* 1985; Todd *et al.* 1988; Brown *et al.* 2017). The frequency, size, water depth, and distribution of scours can provide insight into the extent, dynamics, and geometry of past ice sheets – e.g., wide u-shaped scours are often associated with tabular icebergs calved from ice shelves. Buried scours are observed along the entire margin, except for offshore Troms, however, given their prevalence on the contemporary seafloor (Rydningen *et al.* 2013), it is likely buried examples exist, but have not been mapped due to the limited availability of 3D seismic data. In the Barents Sea, buried and seafloor scours have been mapped, with features typically several kilometres long, with widths and depths up to 50 m and 5 m, respectively (Piasecka *et al.* 2016; Newton and Huuse 2017a; Bellwald *et al.* 2018, 2019). Their morphology is a combination of v-and u-shaped cross-sectional profiles that are accompanied by adjacent berms containing the excavated materials. There is also evidence of scours displaying parallel conformity, suggesting either multi-keel icebergs or an ice melange (Bellwald *et al.* 2019). On the mid-Norwegian margin, the extensive coverage of 3D reflection seismic data have led to the documentation of thousands of iceberg scours. Some of the largest measure up to 500 m wide and 50 km long, but they typically measure 100-200 m wide, 1-5 km long, and ~10-30 m deep. Similar to the Barents Sea, these features have v- and u-shaped cross-sections, with a range of linear, curvilinear, and spiral longitudinal profiles (Fig. 7a). Scours are observed in all Naust units, on both palaeo-shelves and upper palaeo-slopes (Montelli *et al.* 2018a; Newton *et al.* 2018). In the northern North Sea, iceberg scours of similar dimensions to elsewhere on the margin are observed on multiple palaeo-shelf reflections within Unit D (Bellwald *et al.* 2022) (Fig. 7b). Erosion of the older glacigenic stratigraphy by the Norwegian Channel Ice Stream, mean they are only preserved on Middle-Late Pleistocene surfaces (Batchelor *et al.* 2017). In the central and southern North Sea, scours have been extensively mapped on many Early Pleistocene seismic horizons that are partly age-constrained by borehole A15-03 (Fig. 7c-7d) (Dowdeswell and Ottesen 2013; Rea *et al.* 2018).

4.3.2. Proglacial meltwater channels

Proglacial channels tend to behave more dynamically than their fluvial counterparts due to the dominance of seasonal meltwater and its interaction with flushing of the subglacial environment during periods of high melt. These channels typically transport large volumes of material, often with coarser grain sizes, that typically result in braided proglacial channel systems (Maizels 2002). Proglacial meltwater channels are uncommon offshore northwest Europe, though they have been observed. In the southwest Barents Sea, Early Pleistocene channels measuring up to ~20 m deep, with associated channel bars, are observed within a 25 km long and 1-3 km wide glacial valley (Bellwald *et al.* 2021) (Fig. 6a). The valley was first formed by outburst floods from a dammed glacial lake before a proglacial braided river system later occupied the valley when discharge decreased (Bellwald *et al.* 2021).

Within the Naust Formation, new channel-like features have been documented with two different types of morphology – those described above as tunnel valleys, and those discussed below. Channels within Naust T are up to ~6 km long, ~400 m wide, and ~15 m deep (Fig. 6f) follow the local slope gradient and do not have undulating thalwegs, suggesting they formed subaerially. They are also associated with small fan-like features that may represent deposition proximal to the ice sheet margin, suggesting that these channels may be proglacial. In the northern North Sea, the Sunnfjord Channel (Fig. 6c) has been documented at the base of the glacial succession (Løseth *et al.* 2020). In contrast to the ice-adjacent channels described above, this channel is suggested to have been significantly downstream of the ice margin and reflects enhanced seasonal meltwater production during the earliest stages of glaciation in the Norwegian mountains (Løseth *et al.* 2020). As discussed above, while tunnel valleys are common in the North Sea, proglacial channels appear to be less so, though there are examples in the upper stratigraphy of the Dogger Bank area (Emery *et al.* 2019). There is abundant evidence for terrestrial channels on palaeo-shelves in the south and central North Sea, but these relate to non-glacigenic processes – specifically the Rhine-Meuse and Baltic rivers systems (Harding 2015; Lamb *et al.* 2018). The Troms region is the only area with no documentation of channel-like features buried on palaeo-shelves.

4.3.3. Slope features – gullies, channels, and glacigenic debris flows

Most glaciated margins have gullies on the upper continental slope, particularly at the mouth of cross-shelf troughs. They are generally deeper (tens of metres) than they are wide and are often related to sediment-laden subglacial meltwater, tidal-flows, or bottom currents (Ó Cofaigh *et al.* 2003; Gales *et al.* 2014). While gullies may transition into full slope channel systems, they can be differentiated from channels, which often have levee deposits and become wider, deeper, and more sinuous down-dip (Gales *et al.* 2014; Newton *et al.* 2021). Glacigenic debris flows (GDFs) can be associated with gullies and are formed from gravity-driven movement of subglacial materials delivered to the outer shelf (King *et al.* 1996; Taylor *et al.* 2002). In some areas of the margin, canyonisation has taken place and is associated with glacial meltwater and slope failure (Rise *et al.* 2013).

Along the northwest European margin there are extensive observations of gullies and GDFs. In the southwestern Barents Sea, within Units Gi and Gii (Fig. 2), gullies hundreds of metres wide and tens of metres deep have been associated with channelised meltwater (Laberg *et al.* 2010; Waage *et al.* 2018). Unit Gii preserves the first GDF deposits, which become more common during deposition of Unit Giii, where individual mounds measure up to 24 km wide, 50 m thick, and 100 km long. While GDF occurrence increases in the youngest unit, gullies become less common through time (Laberg and Vorren 1995; Laberg *et al.* 2010). Offshore Troms, Unit S2 contains similar lobate deposits that cut into the base Pleistocene surface (Rydningen *et al.* 2016). Within Units S3 and S4, GDFs likely evolved into downslope turbidity currents due to the steep dip of the palaeo-slope, using pre-existing gully-channel complexes to facilitate sediment bypass of the trough mouth fan (Rydningen *et al.* 2016). Offshore Lofoten-Vesterålen, the steep slope margin (up to 3-8 °) led to development of numerous canyons. While canyon initiation may have pre-dated Plio-Pleistocene glaciation, glacial-interglacial cycles of sedimentary processes likely rejuvenated or infilled some canyons – e.g., retrogressive slope failure in the Andøya Canyon (Fig. 1a) was aided by failure of glacigenic sediments delivered to the shelf edge and subsequent turbidity current erosion (Laberg *et al.* 2007; Rise *et al.* 2013).

On the mid-Norwegian margin, gullies, channels, and GDF deposits have been documented on the palaeo-slopes of all Naust units (Montelli *et al.* 2018b). Within Naust U, S, and T, v-shaped gullies up to 750 m wide, 20 m deep, and several kilometres long have been documented. Larger channels up to 20 km long and 1 km wide are most common on the middle and upper palaeo-slopes Naust N, A, and U. They display complex morphology, with individual and bifurcating channels, as well as changes in width and depth associated with localised slope failure (Montelli *et al.* 2018b). In Units U, S, and T, slope deposition largely consists of GDFs (Fig. 8b). In the northern North Sea, GDFs up to 10 km long and 2 km wide are documented on palaeo-slopes of Units A to D (Nygård *et al.* 2005; Batchelor *et al.* 2017; Løseth *et al.* 2020) (Fig. 8c). In the northern North Sea, GDF deposits appear to be the dominant sedimentary process that initially infilled the basin. By the time the North Sea trough-mouth fan was being formed, stacked channel-levee deposits provide evidence for long-distance sediment transport into the Norwegian Sea (Fig. 8a) (Bellwald *et al.* 2020). Further south, in the North Sea the prevalence of slope features is dependent on the location and time period (Batchelor *et al.* 2017; Lamb *et al.* 2017; Ottesen *et al.* 2018). In the southern and central North Sea, channels observed on Early Pleistocene palaeo-slopes are not directly glacial in origin but are instead related to progradation of the Baltic and Rhine Meuse delta front systems and their associated high sediment fluxes and downslope transfer of material (Harding 2015; Lamb *et al.* 2018). In the central North Sea, through time these delta front processes evolved towards a more glacial origin with an increase in glacifluvial sedimentation that helped to infill the basin by the onset of the Middle Pleistocene Transition (Ottesen *et al.* 2018).

5. Ice sheet history of the glacigenic sequences offshore northwest Europe

The seismic geomorphology of the European glaciated margin reveals a suite of landforms that have contributed to revolutionising our understanding of the characteristics of Pleistocene glaciations (Fig. 9). Traditionally, our knowledge was largely based on piecemeal landform observations that were placed within the structure of the global $\delta^{18}O$ sea level record and the assumption that ice sheet changes in North America were the dominant cause of sea level fluctuations (Lisiecki and Raymo 2005; Spratt and Lisiecki 2016). The northwest European record of buried glacial landforms, especially those within Early Pleistocene strata, paints a more complex picture of glaciation than has been previously assumed – with potential implications for our understanding of longer-term records of climate change.

5.1. Ice sheet reconstructions

The southwest Barents Sea region and offshore Troms are the least documented parts of the margin due to limited 3D seismic coverage. It was originally viewed that full glacial conditions did not occur in either region until ~1.5 Ma when observations of GDFs increase (Andreassen *et al.* 2007; Knies *et al.* 2009; Laberg *et al.* 2010; Rydningen *et al.* 2016). This increase, combined with the highly progradational architecture and reduced observations of gullies through time, suggest the gradual intensification of glaciation from ~1.5 Ma as the climate became increasingly polar, with the end result being ice streams crossing the shelf during most, if not all, glacial periods from ~0.7 Ma (Laberg and Vorren 1995; Laberg *et al.* 2010; Rydningen *et al.* 2016; Hjelstuen and Sejrup 2021; Lien *et al.* 2022). Prior to ~1.5 Ma, glaciation of the area was thought to be largely restricted to the mountains and land, with ice sheet margins only occasionally advancing far enough to facilitate a glacifluvial influence on marine depositional patterns (Butt *et al.* 2000; Knies *et al.* 2009; Laberg *et al.* 2010; Rydningen *et al.* 2016; Waage *et al.* 2018). However, MSGLs documented on newly available 3D seismic data covering the Bjørnøyrenna Trough Mouth Fan have pushed the age of shelf edge glaciation back to the onset of the Pleistocene (Harishidayat *et al.* 2021). The MSGL do not allow determination of where the parent ice sheet was centred, but they do provide evidence for extensive glaciation. Offshore Troms, GDF deposits cutting into the base of the Pleistocene succession also suggest an ice sheet reached the palaeo-shelf edge during the earliest Pleistocene (Rydningen *et al.* 2016).

Evidence of buried glacial landforms throughout the Naust Formation suggest that ice regularly advanced onto the shelf from ~2.8 Ma (Dowdeswell *et al.* 2006; Montelli *et al.* 2017, 2018a, b; Newton *et al.* 2018). Tentative evidence for a set of MSGL atop a glacial unconformity are inferred to date to ~1.9 Ma (Newton 2017), while more robust evidence of MSGL suggest fast-flowing ice occurred on the outer palaeo-shelf from at least ~1.6 Ma (Montelli *et al.* 2017) which is matched by increased sedimentation rates (Hjelstuen and Sejrup 2021; Lien *et al.* 2022). Prior to ~1.6 Ma, IRD evidence shows marine-terminating ice in the area from ~2.8 Ma, which is supported by observations of buried channel-gully systems on the slope as ice regularly delivered sediment-laden meltwater to the palaeo-shelf edge (Montelli *et al.* 2018b). The late Pliocene onset of glacial processes on the continental shelf is supported by core evidence documenting sediments of glacimarine and grounded ice origin close to the base Naust (Ottesen *et al.* 2009, 2012). It is suggested that through the Pleistocene, the erosivity of the ice sheets crossing the mid-Norwegian shelf increased as ice streaming became a more common feature (Montelli *et al.* 2018b). Similar to further north, channel-gully systems of the Pleistocene become less frequent through time as GDFs become more common, suggesting an increasing role of subglacial materials delivered directly to the shelf edge and a reduced proportion of sedimentation related to glacimarine processes (Ottesen *et al.* 2012; Montelli *et al.* 2017, 2018b; Newton and Huuse 2017b). Additionally, observations of iceberg scours cover the full period of glaciation on the mid-Norwegian margin since ~2.8 Ma (Newton *et al.* 2016, 2018; Montelli *et al.* 2018a). While unequivocally confirming the icebergs were locally-calved is not possible, the documentation of scours on the upper parts of the palaeo-slopes and outer palaeo-shelves suggests icebergs would have required maintenance of deep drafts if they travelled from elsewhere. The simplest explanation that the icebergs were locally-sourced from ice advancing beyond the coastlines of Norway and/or the British Isles (Montelli *et al.* 2018a; Newton *et al.* 2018) is consistent with IRD of European provenance through many Pleistocene glacial stages (Eidvin *et al.* 2000; Jansen *et al.* 2000; Thierens *et al.* 2012).

In the North Sea, numerous glacigenic landforms have been observed from subglacial and proglacial environments and there are debates on how these buried landform records should be interpreted in relation to Early Pleistocene glaciation, not least of all between some authors on this paper (Ottesen *et al.* 2014, 2018; Batchelor *et al.* 2017; Rea *et al.* 2018; Lloyd *et al.* 2021a; Løseth *et al.* 2022). There are two main interpretations of Early Pleistocene North Sea glaciation: 1) extensive ice sheets from at least ~2.5 Ma; and 2) more restricted ice sheets until at least ~1.2 Ma. Rea *et al.* (2018) combine buried landforms with core data from the Aviat gas field (Rose *et al.* 2018) and a coupled numerical ocean-climate model to propose that the landform record of iceberg scours on many of the clinoform packages in the southern North Sea can only be explained if marine-terminating ice was present in the North Sea Basin from the onset of the Pleistocene. From ~1.87 Ma onwards there are repeated observations of grounded and floating ice landforms (Dowdeswell and Ottesen 2013; Ottesen *et al.* 2014, 2018; Buckley 2017; Rea *et al.* 2018). Rea *et al.* (2018) document numerous sets of MSGL that have been linked to multiple glacial stages throughout the infill of the basin and they interpret this as support for ice sheet extent in the Early Pleistocene potentially being comparable to the Late Pleistocene.

Ottesen *et al.* (2018) mapped glacial landforms and contouritic deposits, proposing that glaciation was more restricted in the North Sea during the Early Pleistocene, with an ice sheet likely only over Norway during glacials. The contouritic deposits are thought to represent water circulation that would have resulted in southward iceberg trajectories into the North Sea – contrasting the interpretation of Rea *et al.* (2018), who proposed northward trajectories taking icebergs out of the North Sea. While Ottesen *et al.* (2018) document GDFs in the earliest seismic units, suggesting ice terminating at the palaeo-shelf break in the northern North Sea from as early as ~2.6 Ma, they propose that major advance of ice into the central North Sea, similar to the Late Pleistocene, only began from the onset of the Middle Pleistocene Transition at ~1.2 Ma, when MSGL are documented at the top of Clinoform Unit 3 (Ottesen *et al.* 2018; Reinardy *et al.* 2018).

Although the timing and extent of any advances are poorly-constrained, Ottesen *et al*. (2018) suggest this evidence of extensive ice is younger than that proposed by Rea *et al.* (2018), but still pre-dates formation of the Norwegian Channel (Ottesen *et al.* 2018). The Norwegian Channel itself is now having the age of its inception challenged from the original ~1.1 Ma age (Sejrup *et al.* 1995) to a younger age of ~0.8 Ma, with sediment deposition in the channel perhaps not occurring until ~0.35 Ma (Løseth *et al.* 2022). Within Unit D, in particular above the NS-URU, iceberg scours, MSGLs, and a glacial outwash fan are associated with the Norwegian Channel Ice Stream (Sejrup *et al.* 2000; Rise *et al.* 2004; Nygård *et al.* 2005; Batchelor *et al.* 2017; Bellwald *et al.* 2022). The presence of older landforms indicative of ice sheet activity are limited by erosion of most Early Pleistocene palaeo-shelves. The top of the Central Basin Unit is interpreted as the NS-URU equivalent and merges with an unconformity in the southern North Sea related to Middle Pleistocene glaciation (Moreau *et al.* 2012; Ottesen *et al.* 2018). This younger stratigraphy of the North Sea (i.e. sediments above the NS-URU equivalent) contains multiple generations of tunnel valleys, glacitectonic deformation structures, and till layers, all indicating extensive glaciation (Huuse and Lykke-Andersen 2000b, a; Stewart and Lonergan 2011; Moreau *et al.* 2012; Bendixen *et al.* 2018).

As outlined above, there is compelling landform evidence along the entire northwest European margin for Early Pleistocene glaciation. It is unequivocal that, notwithstanding dating uncertainties, and limitations in landform preservation and imaging, ice was regularly present on the continental shelves of northwest Europe during Early Pleistocene glacials. While this is supported by IRD of Fennoscandian and the British Isles provenance (Jansen *et al.* 2000; Thierens *et al.* 2012), this is caveated by the notion that IRD does not necessarily mean extensive ice sheets – e.g., calving margins could be close to the coastline, or anchor sea ice transport – the landform evidence provides conclusive evidence of ice sheet influence on outer palaeo-shelves of the Early Pleistocene. Whether this evidence represents contiguous ice margins with coeval maximum extent timelines, or time-transgressive ice margins, perhaps across different glacial stages, is unknown due to limitations in landform continuity and dating. Such observations challenge our wider knowledge of Early Pleistocene climatic and sea level changes.

In the North Sea, different interpretations of landform records have suggested ice advanced beyond only the Norwegian coastline during the Early Pleistocene (Ottesen *et al.* 2018), or both Norway and the British Isles (Rea *et al.* 2018). The resolution of current dating constraints could feasibly mean both interpretations are plausible and may reflect different glacial stages. In the case of the former, this raises questions about what conditions would facilitate build-up of ice over Fennoscandia but not the British Isles. In the case of the latter, this raises questions about how much of the global sea level lowstands of the Early Pleistocene could be attributable to northwest European ice sheets. If both scenarios occurred, this leaves further questions about what differed between different glacial stages to allow such different ice sheet configurations to evolve.

While unravelling the more complete records of recent glaciations in Europe is understandably a key priority, a better knowledge of European ice sheet evolution across longer timescales brings the opportunity to explore how and why ice sheets form and evolve under different orbital and insolation settings. Such results can help elucidate, constrain, and validate numerical models investigating broad processes of ice sheet evolution and its impact on the oceans. For example, can the Pleistocene evolution of the Norwegian Atlantic Current (Montelli *et al.* 2018a; Newton *et al.* 2018) or the evolution of sedimentation rates (Lien *et al.* 2022) be captured in numerical models? This is an increasingly important component of palaeo-climate studies, but remains somewhat disjointed in how modellers can best use the empirical data, and how the empirical community can best use the modelled outputs. The distribution of meltwater landforms is another obvious example – many formed in the North Sea and few in the Norwegian Sea. Some empirical work has proposed explanations for this variation and how it may relate to adjacent open waters (e.g., Newton and Huuse 2017b), but it has not been quantitatively tested. Models capable of recreating ice sheet geometry and sedimentation patterns may then provide insight on how and why landform records vary. More broadly, such multi-disciplinarity may provide information on how ancient ice sheets interacted, responded, and possibly triggered changes in global climate and ocean systems – e.g., the configuration of Northern Hemisphere ice sheets will influence the polar front and storm tracks. The position of storm tracks then has a knock-on effect on precipitation and temperature patterns, impacting not just mass balance of any ice sheets, but the biosphere in non-glacial regions. Thus, the landform records have the potential to contribute beyond simple locations of fast-flowing ice.

5.2. Global glaciation and the Early Pleistocene world

In a global context, the above considerations are especially interesting when thinking about how ice sheets are reflected in the oxygen isotope record, and why the global climate system switched from a 41-kyr to a 100-kyr-world during the Middle Pleistocene Transition. While erosion/deposition through multiple glaciations means reconstructing Early Pleistocene ice sheets is problematic (Ehlers *et al.* 2011), there is an array of evidence. In North America, the Laurentide Ice

Sheet reached as far south as 39 °N at ~2.4 Ma (Balco and Rovey 2010). The geomorphological record suggests the Laurentide did not reach this latitude again for ~1 Myr, but inferences on ice sheet size from meltwater pulses observed in the Gulf of Mexico suggest that prior to ~1.7 Ma there were at least six occasions when the ice sheet reached the mid-latitudes (Shakun *et al.* 2016). In Alberta, Canada, borehole magnetic data suggest the ice sheet margin was at least 300 km further west in the Early Pleistocene than previously thought (Andriashek and Barendregt 2017). Extensive glaciation is also observed in ocean cores from the North Pacific and North Atlantic, suggesting that Early Pleistocene ice in the west and east reached the coastline (Krissek 1995; Bailey *et al.* 2013; Hidy *et al.* 2013). Cores from the North Pacific also document IRD from the Kurile/Kamchatka margin in Russia (Krissek 1995), while glaciation in eastern Artic Russia is documented through deposition of glacial tills dated to 3.5-3.2 Ma and 2.5-2.4 Ma (Laukhun *et al.* 1999).

Recent geophysical work offshore northwest Greenland documented numerous unconformities reflecting ice advances to palaeo-shelf edges from the late Pliocene onwards (Knutz *et al.* 2019; Newton *et al.* 2020, 2021). In Disko Bay, the sedimentary succession suggests the onset of offshore ice advance during the late Pliocene and Early Pleistocene (Hofmann *et al.* 2016). Offshore south Greenland there is support for shelf edge glaciation from 2.5-2.0 Ma (Nielsen and Kuijpers 2013) and as far back as ~7 Ma (Larsen *et al.* 1994). In east Greenland, similar data show offshore ice at the onset of the Pleistocene and frequent advances thereafter (Laberg *et al.* 2013; Pérez *et al.* 2018). In northeast Greenland, increased progradation occurred at ~2.5 Ma and is linked with ice advance (Berger and Jokat 2009). Geological records from beneath the Greenland Ice Sheet and numerical modelling are challenging to interpret, but in all scenarios authors suggest an ice sheet was likely present during glacials (which correlates with the offshore record and IRD), with the main uncertainty pertaining to ice volume and extent in the intervening interglacials (Solgaard *et al.* 2011; Bierman *et al.* 2016; Schaefer *et al.* 2016). Elsewhere in the Northern Hemisphere, glacigenic deposits in Iceland suggest regional ice cover from the onset of the Pleistocene, with major, island-wide, glaciation from ~2.2 Ma and numerous times afterward (Geirsdóttir and Eiríksson 1994; Geirsdóttir *et al.* 2007). In the European Alps, the evidence is sporadic, but there is support for numerous Early Pleistocene glaciations (Muttoni *et al.* 2003; Preusser *et al.* 2011). In the Himalayas there is limited research on Early Pleistocene glaciation, but there is evidence of some tills and glacifluvial deposits (Benxing 1988; Benxing and Rutter 1998; Abramowski *et al.* 2006).

In South America, expansive glaciation during the Early Pleistocene, in particular the Great Patagonian Glaciation, is indicated by meltwater deposits and ice-margin landforms thought to date to the earliest Pleistocene (Coronato *et al.* 2004a, b; Rabassa 2008), as well as till units intercalated with lava flows showing at least seven glaciations from 2.1-1.1 Ma (Clague *et al.* 2020). In Africa, smaller ice covers developed in areas like Mount Kilimanjaro, where glaciation is thought to have begun at ~2.0 Ma (Mahaney 2004). Australia had its largest ice cover in the Early Pleistocene (Colhoun and Barrows 2011), while in New Zealand the extensive ice cover of the Ross Glaciation of the South Island is thought to date to 2.6-2.4 Ma (Suggate 1990; Barrell 2011; Newnham *et al.* 2016). Finally, in Antarctica, though the sedimentary record suggests a general level of stability (Hillenbrand and Ehrmann 2005; Bailey *et al.* 2022), there is clear seismic evidence for numerous advances of ice onto the continental shelf during the Early Pleistocene (Smith and Anderson 2010; Davies *et al.* 2012).

The evidence presented above is not exhaustive, but it is enough to raise questions on how well we understand Early Pleistocene climate history. Landform and sedimentary records provide unequivocal evidence of glaciation across numerous areas during this time. Such an observation perhaps challenges the global sea level record, or at least implicit assumptions that are based upon it (e.g., Laurentide dominance). For example, how can we have Early Pleistocene ice sheets in North America and Europe that are potentially comparable in size to those in the Middle-Late Pleistocene, when sea level lowstands during the 41-kyr-world were only 50-60 % the magnitude of those in the 100-kyr-world? Some authors propose the discrepancies can be explained by extensive regolith facilitating 'low-slung' ice sheets – i.e., ice reached areal extents similar to those of the Late Pleistocene, but by being thinner they maintained a smaller volume (Rea *et al.* 2018). Earth-system modelling of how regolith and CO_2 evolved through the Pleistocene match well with the sea level record and also the switch from a 41-kyr-world to a 100-kyr-world (Willeit *et al.* 2019), but the results are yet to accurately capture the extent and distribution of several ice sheets documented from sedimentary and seismic records. If the sea level record is correct, then one possibility is that different glacial stages of the Early Pleistocene were characterised by a variation in how the different ice sheets accounted for ice volumes – i.e., while the Laurentide Ice Sheet may have been largely dominant, perhaps its impact on global sea level is not uniform across numerous glacial stages and different ice sheets provided variable contributions through time. Recent cosmogenic nuclide work on IRD associated with the Laurentide suggests the ice sheet may have been more persistent during some Pleistocene interglacials than previously thought (LeBlanc *et al.* 2023), adding further uncertainty to our knowledge of interglacials, not just glacials.

Collectively, the traditional view that the magnitude of glaciation gradually increased from smaller ice sheets in the Early Pleistocene to larger ice sheets in the Middle-Late Pleistocene, is being increasingly challenged by new data – as shown in this paper, the date for the earliest grounded ice on northwest European palaeo-shelves has been regularly pushed back in time. Where the answer for resolving this can be found is difficult to know, but it is possible that during the Early Pleistocene the ocean $\delta^{18}O$ record was not always fully coupled with ice sheet behaviour, or, perhaps more likely, there are issues, such as post-deposition modification, that impact how effective current geochemical methods are for extracting past sea level fluctuations, in particular the magnitude of sea level changes. Regardless of whether the isotope record provides a sufficiently robust characterisation of the Early Pleistocene or not, geological records suggest that major ice sheets have repeatedly come and gone during the 41-kyr-world. Given the gradual decline in CO_2 levels through the Pleistocene, the potential for rapidly changing ice sheets at times when CO_2 was potentially comparable to contemporary levels, provides intrigue on how responsive ice sheets may have been in the past, particularly if they were able to attain much larger extents and volumes than currently indicated by the $\delta^{18}O$ record.

5.3. Future research

The increased availability of legacy and new reflection seismic data are likely to continue adding new evidence of Early Pleistocene glaciations. A key research need is, therefore, to attach greater geochronological control to these landforms and the glacigenic stratigraphy that they are documented within. While there are some age constraints along the margin (Fig. 2), these have been derived from a small number of older boreholes, with the materials rarely subjected to modern methods. This is reflected by the fact that over the last ~30 years, some of the ages for the different units have changed when reanalysed (e.g., the Naust Formation). The variable facies of these glacigenic sequences provides additional complications because reworked sediments with a paucity of dates from a limited number of borehole sites, means that any correlation between different sequences is challenging. Seismic stratigraphy does help with correlation, but it is important to consider the difference in scale between not just the resolution of different vintages of reflection seismic data, but also with borehole data. There is also the implicit assumption built into seismic interpretation that amplitude reflections represent geological timelines, which is not guaranteed to be the case, particularly if the vertical resolution is low. It is only in the southern North Sea where the earliest part of the Pleistocene has good age control, with the caveat that, even here, the chronostratigraphy is insufficient for isolating individual glacial-interglacial cycles.

While the broad-scale of the ideas presented in this discussion are not significantly impacted by the quality and quantity of core materials – the buried landform records are clearly of Early Pleistocene age – it does provide a limiting factor on how much detail can be attached to the palaeo-glaciological reconstructions. This limitation is easily observed on the European glaciated margin, where the ice sheet reconstructions are not just contested, but also have potential to significantly impact global sea level reconstructions. Key uncertainties remain about how extensive the ice was in Fennoscandia and the British Isles during the Early Pleistocene, when grounded ice first reached the centre of the North Sea, when and how often the two ice sheets coalesced in the North Sea, when and how ice on Svalbard coalesced with ice in northern Norway in the Barents Sea, how the transition from the 41-kyr-world to the 100-kyr-world was represented in northwest Europe, and when and how ice sheet processes were impacted by the removal and eventual exhaustion of regolith.

The glacigenic stratigraphy of northwest European is the best documented glaciated margin in the world and developing an improved chronology, alongside better documentation of facies variations along the margin, would ground-truth the reflection seismic interpretations and help elucidate answers to the uncertainties outlined above. Providing greater clarity about regional changes is also important for understanding how they fit within and impact the wider framework of global glaciation through the Pleistocene. Furthermore, such an undertaking would have an applied impact on not just the siting of windfarms, but also the investigation of carbon sequestration. This is because a number of areas currently identified for potential carbon storage on the European margin are overlain by significant thicknesses of glacigenic stratigraphy and questions exist over the impact of heterogeneities and flow/thief units on the sealing capacity of the Pleistocene succession and the efficacy of CO_2 storage targets (Lloyd *et al.* 2021a, b). The wealth of evidence provided by conventional seismic data released from industrial operations in the oil and gas sector of the North Sea demonstrates the scientific value of such data and the need to maintain access and data integrity for future study. It also demonstrates how scientifically useful a similar release mechanism for newer, high resolution data acquired for carbon storage and wind farm purposes would be for analyses of the shallow glacigenic stratigraphy and the climatic information that it contains.

6. Conclusion

Geological data from boreholes offshore northwest Europe have shown that the landscape has experienced the waxing and waning of ice sheets since the late Pliocene. While data from these boreholes, such as IRD, provide a good understanding on the presence of ice, it provides little in the way of insight on the extent, magnitude, and ice dynamics during those periods of glaciation. This is especially the case for glaciations preceding the last one. Basin-scale stratigraphic analyses from 2D seismic data have provided a framework that can be linked to broad changes in depositional styles, but the real step forward has come from the application of 3D seismic data within that framework. These data provide the ability to capture an array of glacial landforms buried beneath the contemporary continental shelves of northwest Europe. Cataloguing of such landforms, as presented here, provides the opportunity to explore how the nature of glaciation has evolved through time.

While imaging resolution, preservation potential, and large-scale glacial erosion provide limitations on how much information can be extracted from the subsurface, it has revolutionised our understanding of glaciation history. We see from more recent records that the earliest grounded glaciation has repeatedly been pushed back into the earliest parts of the Pleistocene along different parts of the margin (Montelli *et al.* 2018b; Rea *et al.* 2018; Harishidayat *et al.* 2021). These observations, combined, have tended to result in more questions arising than being answered, such as, what does the Early Pleistocene landform record of the North Sea really mean for ice sheet reconstruction – if, as currently, the glacial reconstructions from the landforms vary so considerably?

The landform records of northwest Europe and other glaciated margins, when considered together, begin to challenge the efficacy of the global oxygen isotope record. Across most glaciated margins, there is evidence for extensive glaciation at some stages during the Early Pleistocene and it has become increasingly difficult to conceptualise how so many large ice sheets can be captured by sea level lowstands magnitudes only 50-60 % of those in the Middle-Late Pleistocene. It also raises important questions about the speed at which ice sheets disappeared in the 41-kyr-world. Undoubtedly, a key step in taking these results forward is to begin to attach greater chronological control, with the hope of exploring in more detail the origin of these features, the spatio-temporal continuity of the landform records, and how they relate to global climatic changes.

Acknowledgements

AMWN was supported by the Natural Environment Research Council (NERC grant reference number NE/K500859/1 and NE/R013675/1) and Cairn Energy. Schlumberger, Eliis, and ESRI are thanked for providing Petrel, Paleoscan, and ArcGIS software, respectively. Data provided courtesy of the Norwegian Petroleum Directorate, Spectrum ASA, OGA, and WesternGeco. AMWN thanks Ted Newton for constructive discussions during manuscript preparation. The authors are grateful to the two reviewers and editor for comments that improved manuscript clarity.

References

Abramowski, U., Bergau, A., Seebach, D., Zech, R., Glaser, B., Sosin, P., Kubik, P.W. and Zech, W. 2006. Pleistocene glaciations of Central Asia: results from 10Be surface exposure ages of erratic boulders from the Pamir (Tajikistan), and the Alay–Turkestan range (Kyrgyzstan). Quaternary Science Reviews, 25, 1080–1096, https://doi.org/10.1016/J.QUASCIREV.2005.10.003.

Alexandropoulou, N., Winsborrow, M., Andreassen, K., Plaza-Faverola, A., Dessandier, P.A., Mattingsdal, R., Baeten, N. and Knies, J. 2021. A Continuous Seismostratigraphic Framework for the Western Svalbard-Barents Sea Margin Over the Last 2.7 Ma: Implications for the Late Cenozoic Glacial History of the Svalbard-Barents Sea Ice Sheet. Frontiers in Earth Science, 9, 327, https://doi.org/10.3389/FEART.2021.656732/BIBTEX.

Andreassen, K. and Winsborrow, M. 2009. Signature of ice streaming in Bjørnøyrenna, Polar North Atlantic, through the pleistocene and implications for ice-stream dynamics. Annals of Glaciology, 50, 17–26, https://doi.org/10.3189/172756409789624238.

Andreassen, K., Nilssen, L.C., Rafaelsen, B. and Kuilman, L. 2004. Three-dimensional seismic data from the Barents Sea margin reveal evidence of past ice streams and their dynamics. Geology, 32, 729–732, https://doi.org/10.1130/G20497.1.

Andreassen, K., Ødegaard, C.M. and Rafaelsen, B. 2007. Imprints of former ice streams, imaged and interpreted using industry three-dimensional seismic data from the south-western Barents Sea. In: Davies, R. J., Posamentier, H. W., Wood, L. W. and Cartwright, J. A. (eds) Seismic Geomorphology: Applications to Hydrocarbon Exploration and Production. Geological Society, London, Special Publication, 277, 151–169., https://doi.org/10.1144/GSL.SP.2007.277.01.09.

Andriashek, L.D. and Barendregt, R.W. 2017. Evidence for Early Pleistocene glaciation from borecore stratigraphy in north-central Alberta, Canada. Canadian Journal of Earth Sciences, 54, 445–460, https://doi.org/10.1139/cjes-2016-0175.

Bailey, I., Hole, G.M., Foster, G.L., Wilson, P.A., Storey, C.D., Trueman, C.N. and Raymo, M.E. 2013. An alternative suggestion for the Pliocene onset of major northern hemisphere glaciation based on the geochemical provenance of North Atlantic Ocean ice-rafted debris. Quaternary Science Reviews, 75, 181–194, https://doi.org/10.1016/J.QUASCIREV.2013.06.004.

Bailey, I., Hemming, S., Reilly, B.T., Rollinson, G., Williams, T., Weber, M.E., Raymo, M.E., Peck, V.L., Ronge, T.A., Brachfeld, S., O'Connell, S., Tauxe, L., Warnock, J.P., Armbrecht, L., Cardillo, F.G., Du, Z. Fauth, G., Garcia, M., Glueder, A., Guitard, M., Gutjahr, M., Hernández-Almeida, I., Hoem, F.S., Hwang, J.H., Iizuka, M., Kato, Y., Kenlee, B., Martos, Y.M., Pérez, L.F., Seki, O., Tripathi, S. and Zheng, X. 2022. Episodes of Early Pleistocene West Antarctic Ice Sheet Retreat Recorded by Iceberg Alley Sediments. Paleoceanography and Paleoclimatology, 37, e2022PA004433, https://doi.org/10.1029/2022PA004433.

Balco, G. and Rovey, C.W. 2010. Absolute chronology for major Pleistocene advances of the laurentide ice Sheet. Geology, 38, 795–798, https://doi.org/10.1130/G30946.1.

Balco, G., Rovey, C.W. and Stone, J.O.H. 2005. The first glacial maximum in North America. Science, 307, 222, https://doi.org/10.1126/science.1103406.

Barr, I.D. and Lovell, H. 2014. A review of topographic controls on moraine distribution. Geomorphology, 226, 44–64, https://doi.org/10.1016/j.geomorph.2014.07.030.

Barrell, D.J.A. 2011. Quaternary Glaciers of New Zealand. Developments in Quaternary Science, 15, 1047–1064, https://doi.org/10.1016/B978-0-444-53447-7.00075-1.

Batchelor, C.L. and Dowdeswell, J.A. 2015. Ice-sheet grounding-zone wedges (GZWs) on high-latitude continental margins. Marine Geology, 363, 65–92, https://doi.org/10.1016/j.margeo.2015.02.001.

Batchelor, C.L. and Dowdeswell, J.A. 2016. Lateral shear-moraines and lateral marginal-moraines of palaeo-ice streams. Quaternary Science Reviews, 151, 1–26, https://doi.org/10.1016/J.QUASCIREV.2016.08.020.

Batchelor, C.L., Ottesen, D. and Dowdeswell, J.A. 2017. Quaternary evolution of the northern North Sea margin through glacigenic debris-flow and contourite deposition. Journal of Quaternary Science, 32, 416–426, https://doi.org/10.1002/jqs.2934.

Batchelor, C.L., Margold, M., Krapp, M., Murton, D.K., Dalton, AS., Gibbard, P.L., Stokes, C.R., Murton, J.B. and Manica, A. 2019. The configuration of Northern Hemisphere ice sheets through the Quaternary. Nature Communications, https://doi.org/10.1038/s41467-019-11601-2.

Bellwald, B. and Planke, S. 2019. Shear margin moraine, mass transport deposits and soft beds revealed by high-resolution p-cable three-dimensional seismic data in the hoop area, barents sea. In: Lintern, D.G., Mosher, D.C., Moscardelli, L.G., Bobrowsky, P.T., Campbell, C., Chaytor, J., Clague, J., Georgiopoulou, A., Lajeunesse, P., Normandeau, A., Piper, D., Scherwath, M., Stacey, C. and Turmel, D. (eds) Subaqueous Mass Movements. Geological Society, London, Special Publication, 477, 537–547., https://doi.org/10.1144/SP477.29.

Bellwald, B., Planke, S., Polteau, S., Lebedeva-Ivanova, N., Hafeez, A., Faleide, J.I. and Myklebust, R. 2018. Detailed structure of buried glacial landforms revealed by high-resolution 3D seismic data in the SW Barents Sea. In: 80th EAGE Conference and Exhibition 2018. 1–5.

Bellwald, B., Planke, S., Lebedeva-Ivanova, N., Piasecka, E.D. and Andreassen, K. 2019. High-resolution landform assemblage along a buried glacio-erosive surface in the SW Barents Sea revealed by P-Cable 3D seismic data. Geomorphology, 332, 33–50, https://doi.org/10.1016/j.geomorph.2019.01.019.

Bellwald, B., Planke, S., Becker, L.W.M. and Myklebust, R. 2020. Meltwater sediment transport as the dominating process in mid-latitude trough mouth fan formation. Nature Communications2, 11, 4645, https://doi.org/10.1038/s41467-020-18337-4.

Bellwald, B., Planke, S., Polteau, S., Lebedeva-Ivanova, N., Faleide, J.I., Morris, S.M., Morse, S. and Castelltort, S. 2021. Characterization of a glacial paleo-outburst flood using high-resolution 3-D seismic data: Bjørnelva River Valley, SW Barents Sea. Journal of Glaciology, 67, 404–420, https://doi.org/10.1017/JOG.2020.115.

Bellwald, B., Planke, S., Vadakkepuliyambatta, S., Buenz, S., Batchelor, C.L., Manton, B., Zastrozhnov, D., Walker, F., Garcia, A., Myklebust, R. and Kjølhamar, B. 2022. Quaternary and Neogene reservoirs of the Norwegian Continental Shelf and the Faroe-Shetland Basin. First Break, 40, 43–54, https://doi.org/10.3997/1365-2397.FB2022045/CITE/REFWORKS.

Bellwald, B., Stokke, H., Winsborrow, M., Planke, S., Sættem, J., Lebedeva-Ivanova, N., Hafeez, A., Kurjanski, B., Myklebust, R. and Polteau, S. 2023. Structural and fluid-migration control on hill-hole pair formation: Evidence from high-resolution 3D seismic data from the SW Barents Sea. Geomorphology, 420, 108502, https://doi.org/10.1016/J.GEOMORPH.2022.108502.

Bendixen, C., Lamb, R.M., Huuse, M., Boldreel, L.O., Jensen, J.B. and Clausen, O.R. 2018. Evidence for a grounded ice sheet in the central North Sea during the early middle pleistocene donian glaciation. Journal of the Geological Society, 175, 291–307, https://doi.org/10.1144/jgs2017-073.

Benvenuti, A., Šegvić, B. and Moscariello, A. 2018. Tunnel valley deposits from the southern North Sea – material provenance and depositional processes. Boreas, 47, 625–642, https://doi.org/10.1111/BOR.12292.

Benxing, Z. 1988. Quaternary glaciation of Mt. Qomolangma-Xixabangma region. GeoJournal, 17, 525–543, https://doi.org/10.1007/BF00209441/METRICS.

Benxing, Z. and Rutter, N. 1998. On the problem of Quaternary glaciations, and the extent and patterns of Pleistocene ice cover in the Qinghai-Xizang (Tibet) Plateau. Quaternary International, 45–46, 109–122, https://doi.org/10.1016/S1040-6182(97)00009-8.

Berger, D. and Jokat, W. 2009. Sediment deposition in the northern basins of the North Atlantic and characteristic variations in shelf sedimentation along the East Greenland margin. Marine and Petroleum Geology, 26, 1321–1337, https://doi.org/10.1016/J.MARPETGEO.2009.04.005.

Bierman, P.R., Shakun, J.D., Corbett, L.B., Zimmerman, S.R. and Rood, D.H. 2016. A persistent and dynamic East Greenland Ice Sheet over the past 7.5 million years. Nature, 540, 256–260, https://doi.org/10.1038/nature20147.

Bradwell, T., Stoker, M.S., Golledge, N.R., Wilson, C.K., Merritt, J.W., Long, D., Everest, J.D., Hestvik, O.B., Stevenson, A.G., Hubbard, A.L., Finlayson, A.G. and Mathers, H.E. 2008. The northern sector of the last British Ice Sheet: Maximum extent and demise. Earth-Science Reviews, 88, 207–226, https://doi.org/10.1016/j.earscirev.2008.01.008.

Bridges, J.D., Tarduno, J.A., Cottrell, R.D. and Herbert, T.D. 2023. Rapid strengthening of westerlies accompanied intensification of Northern Hemisphere glaciation. Nature Communications 2023 14:1, 14, 1–11, https://doi.org/10.1038/s41467-023-39557-4.

Brown, C.S., Newton, A.M.W., Huuse, M. and Buckley, F. 2017. Iceberg scours, pits, and pockmarks in the North Falkland Basin. Marine Geology, 386, 140–152, https://doi.org/10.1016/j.margeo.2017.03.001.

Buckley, F.A. 2017. A glaciogenic sequence from the Early Pleistocene of the Central North Sea. Journal of Quaternary Science, 32, 145–168, https://doi.org/10.1002/jqs.2867.

Butt, F.A., Elverhøi, A., Solheim, A. and Forsberg, C.F. 2000. Deciphering Late Cenozoic development of the western Svalbard Margin from ODP Site 986 results. Marine Geology, 169, 373–390, https://doi.org/10.1016/S0025-3227(00)00088-8.

Clague, J.J., Barendregt, R.W., Menounos, B., Roberts, N.J., Rabassa, J., Martinez, O., Ercolano, B., Corbella, H. and Hemming, S.R. 2020. Pliocene and Early Pleistocene glaciation and landscape evolution on the Patagonian Steppe, Santa Cruz province, Argentina. Quaternary Science Reviews, 227, 105992, https://doi.org/10.1016/J.QUASCIREV.2019.105992.

Clark, C.D. 1993. Mega-scale glacial lineations and cross-cutting ice-flow landforms. Earth Surface Processes and Landforms, 18, 1–29, https://doi.org/10.1002/esp.3290180102.

Clark, C.D., Tulaczyk, S.M., Stokes, C.R. and Canals, M. 2003. A groove-ploughing theory for the production of mega-scale glacial lineations, and implications for ice-stream mechanics. Journal of Glaciology, 49, 240–256, https://doi.org/10.3189/172756503781830719.

Colhoun, E.A. and Barrows, T.T. 2011. The Glaciation of Australia. Developments in Quaternary Science, 15, 1037–1045, https://doi.org/10.1016/B978-0-444-53447-7.00074-X.

Coronato, A., Martínez, O. and Rabassa, J. 2004a. Glaciations in Argentine Patagonia, southern South America. Developments in Quaternary Science, 2, 49–67, https://doi.org/10.1016/S1571-0866(04)80111-8.

Coronato, A., Meglioli, A. and Rabassa, J. 2004b. Glaciations in the Magellan Straits and Tierra del Fuego, southernmost South America. Developments in Quaternary Science, 2, 45–48, https://doi.org/10.1016/S1571-0866(04)80110-6.

Cox, D.R., Newton, A.M.W. and Huuse, M. 2020. An introduction to seismic reflection data: acquisition, processing and interpretation. In: Scarselli, N., Adam, J., Chiarella, D., Roberts, D.G. and Bally, A.W. (eds) Regional Geology and Tectonics: Volume 1: Principles of Geologic Analysis, Second Edition. Elsevier, 571–603, https://doi.org/10.1016/B978-0-444-64134-2.00020-1.

Dahlgren, K.I.T., Vorren, T.O. and Laberg, J.S. 2002a. Late Quaternary glacial development of the mid-Norwegian margin-65 to 68°N. Marine and Petroleum Geology, 19, 1089–1113, https://doi.org/10.1016/S0264-8172(03)00004-7.

Dahlgren, K.I.T., Vorren, T.O. and Laberg, J.S. 2002b. The role of grounding-line sediment supply in ice-sheet advances and growth on continental shelves: An example from the mid-Norwegian sector of the Fennoscandian ice sheet during the Saalian and Weichselian. Quaternary International, 95–96, 25–33, https://doi.org/10.1016/S1040-6182(02)00024-1.

Dahlgren, K.I.T., Vorren, T.O., Stoker, M.S., Nielsen, T., Nygård, A. and Sejrup, H.P. 2005. Late Cenozoic prograding wedges on the NW European continental margin: Their formation and relationship to tectonics and climate. Marine and Petroleum Geology, 22, 1089–1110, https://doi.org/10.1016/j.marpetgeo.2004.12.008.

Davies, B.J., Hambrey, M.J., Smellie, J.L., Carrivick, J.L. and Glasser, N.F. 2012. Antarctic Peninsula Ice Sheet evolution during the Cenozoic Era. Quaternary Science Reviews, 31, 30–66, https://doi.org/10.1016/J.QUASCIREV.2011.10.012.

Dowdeswell, J.A. and Ottesen, D. 2013. Buried iceberg ploughmarks in the early Quaternary sediments of the central North Sea: A two-million year record of glacial influence from 3D seismic data. Marine Geology, 344, 1–9, https://doi.org/10.1016/j.margeo.2013.06.019.

Dowdeswell, J.A., Ottesen, D. and Rise, L. 2006. Flow switching and large-scale deposition by ice streams draining former ice sheets. Geology, 34, 313–316, https://doi.org/10.1130/G22253.1.

Dowdeswell, J.A., Ottesen, D., Rise, L. and Craig, J. 2007. Identification and preservation of landforms diagnostic of past ice-sheet activity on continental shelves from three-dimensional seismic evidence. Geology, 35, 359–362, https://doi.org/10.1130/G23200A.1.

Dowdeswell, J.A., Ottesen, D., Evans, J., Cofaigh, C.Ó. and Anderson, J.B. 2008. Submarine glacial landforms and rates of ice-stream collapse. Geology, 36, 819–822, https://doi.org/10.1130/G24808A.1.

Dowdeswell, J.A., Canals, M., Jakobsson, M., Todd, B.J., Dowdeswell, E.K. and Hogan, K.A. 2016. Atlas of Submarine Glacial Landforms: Modern, Quaternary and Ancient. Geological Society, London, Memoir, 46, https://doi.org/10.1144/M46.

Ehlers, J., Gibbard, P.L. and Hughes, P.D. 2011. Introduction. Developments in Quaternary Science, 15, 1–14, https://doi.org/10.1016/B978-0-444-53447-7.00001-5.

Eidvin, T., Brekke, H., Riis, F. and Renshaw, D.K. 1998. Cenozoic stratigraphy of the Norwegian Sea continental shelf, 64°N-68°N. Norsk Geologisk Tidsskrift, 78, 125–151.

Eidvin, T., Jansen, E., Rundberg, Y., Brekke, H. and Grogan, P. 2000. The upper Cainozoic of the Norwegian continental shelf correlated with the deep sea record of the Norwegian Sea and the North Atlantic. Marine and Petroleum Geology, 17, 579–600, https://doi.org/10.1016/S0264-8172(00)00008-8.

Emery, A.R., Hodgson, D.M., Barlow, N.L.M., Carrivick, J.L., Cotterill, C.J. and Phillips, E. 2019. Left High and Dry: Deglaciation of Dogger Bank, North Sea, Recorded in Proglacial Lake Evolution. Frontiers in Earth Science, https://doi.org/10.3389/feart.2019.00234.

EMODnet Bathymetry Consortium. 2018. EMODnet Digital Bathymetry (DTM). EMODnet Bathymetry.

Evans, D.J.A. and Rea, B.R. 1999. Geomorphology and sedimentology of surging glaciers: a land-systems approach. Annals of Glaciology, 28, 75–82, https://doi.org/10.3189/172756499781821823.

Faleide, J.I., Solheim, A., Fiedler, A., Hjelstuen, B.O., Andersen, E.S. and Vanneste, K. 1996. Late Cenozoic evolution of the western Barents Sea-Svalbard continental margin. Global and Planetary Change, 12, 53–74, https://doi.org/10.1016/0921-8181(95)00012-7.

Gales, J.A., Leat, P.T., Larter, R.D., Kuhn, G., Hillenbrand, C.D., Graham, A.G.C., Mitchell, N.C., Tate, A.J., Buys, G.B. and Jokat, W. 2014. Large-scale submarine landslides, channel and gully systems on the southern Weddell Sea margin, Antarctica. Marine Geology, 348, 73–87, https://doi.org/10.1016/j.margeo.2013.12.002.

Geirsdóttir, A. and Eiríksson, J. 1994. Growth of an Intermittent Ice Sheet in Iceland during the Late Pliocene and Early Pleistocene. Quaternary Research, 42, 115–130, https://doi.org/10.1006/QRES.1994.1061.

Geirsdóttir, Á., Miller, G.H. and Andrews, J.T. 2007. Glaciation, erosion, and landscape evolution of Iceland. Journal of Geodynamics, 43, 170–186, https://doi.org/10.1016/J.JOG.2006.09.017.

Harding, R. 2015. Evolution of the Giant Southern North Sea Shelf-Prism: Testing Sequence Stratigraphic Concepts and the Global Sea Level Curve With Full-Three Dimensional Control. Phe Thesis, University of Manchester.

Harishidayat, D., Johansen, S.E., Batchelor, C., Omosanya, K.O. and Ottaviani, L. 2021. Pliocene–Pleistocene glacimarine shelf to slope processes in the south-western Barents Sea. Basin Research, 33, 1315–1336, https://doi.org/10.1111/BRE.12516.

Hayashi, T., Yamanaka, T., Hikasa, Y., Sato, M., Kuwahara, Y. and Ohno, M. 2020. Latest Pliocene Northern Hemisphere glaciation amplified by intensified Atlantic meridional overturning circulation. Nature Communications: Earth & Environment, 1, 25, https://doi.org/10.1038/s43247-020-00023-4.

Henrich, R. and Baumann, K.H. 1994. Evolution of the Norwegian Current and the Scandinavian Ice Sheets during the past 2.6 m.y.: evidence from ODP Leg 104 biogenic carbonate and terrigenous records. Palaeogeography, Palaeoclimatology, Palaeoecology, 108, 75–94, https://doi.org/10.1016/0031-0182(94)90023-X.

Hidy, A.J., Gosse, J.C., Froese, D.G., Bond, J.D. and Rood, D.H. 2013. A latest Pliocene age for the earliest and most extensive Cordilleran Ice Sheet in northwestern Canada. Quaternary Science Reviews, 61, 77–84, https://doi.org/10.1016/J.QUASCIREV.2012.11.009.

Hillenbrand, C.D. and Ehrmann, W. 2005. Late Neogene to Quaternary environmental changes in the Antarctic Peninsula region: evidence from drift sediments. Global and Planetary Change, 45, 165–191, https://doi.org/10.1016/J.GLOPLACHA.2004.09.006.

Hjelstuen, B.O. and Sejrup, H.P. 2021. Latitudinal variability in the Quaternary development of the Eurasian ice sheets—Evidence from the marine domain. Geology, 49, 346–351, https://doi.org/10.1130/G48106.1.

Hjelstuen, B.O., Eldholm, O. and Faleide, J.I. 2007. Recurrent Pleistocene mega-failures on the SW Barents Sea margin. Earth and Planetary Science Letters, 258, 605–618, https://doi.org/10.1016/j.epsl.2007.04.025.

Hofmann, J.C., Knutz, P.C., Nielsen, T. and Kuijpers, A. 2016. Seismic architecture and evolution of the Disko Bay trough-mouth fan, central West Greenland margin. Quaternary Science Reviews, 147, 69–90, https://doi.org/10.1016/j.quascirev.2016.05.019.

Holtedahl, H. 1967. Notes on the Formation of Fjords and Fjord-Valleys. Geografiska Annaler. Series A, Physical Geography, 49, 188–203, https://doi.org/10.2307/520887.

Huuse, M. and Lykke-Andersen, H. 2000a. Large-scale glaciotectonic thrust structures in the eastern Danish North Sea. In: Maltman, A. J., Hubbard, B. and Hambrey, M. J. (eds) Deformation of Glacial Materials. Geological Society, London, Special Publication, 176, 393–305., https://doi.org/10.1144/GSL.SP.2000.176.01.22.

Huuse, M. and Lykke-Andersen, H. 2000b. Overdeepened Quaternary valleys in the eastern Danish North Sea: Morphology and origin. Quaternary Science Reviews, 19, 1233–1253, https://doi.org/10.1016/S0277-3791(99)00103-1.

Jansen, E. and Sjøholm, J. 1991. Reconstruction of glaciation over the past 6 Myr from ice-borne deposits in the Norwegian Sea. Nature, 249, 600–603, https://doi.org/10.1038/349600a0.

Jansen, E., Slettemark, B., Bleil, U., Henrich, R., Kringstad, L. and Rolfsen, S. 1989. Oxygen and carbon isotope stratigraphy and magnetostratigraphy of the last 2.8 Ma: Paleoclimatic comparisons between the Norwegian Sea and the North Atlantic. In: Proceedings of the Ocean Drilling Program: Scientific Results. 104, 255–269.

Jansen, E., Fronval, T., Rack, F. and Channell, J.E.T. 2000. Pliocene-pleistocene ice rafting history and cyclicity in the Nordic seas during the last 3.5 myr. Paleoceanography, 15, 709–721, https://doi.org/10.1029/1999PA000435.

King, E.C., Hindmarsh, R.C.A. and Stokes, C.R. 2009. Formation of mega-scale glacial lineations observed beneath a West Antarctic ice stream. Nature Geoscience, 2, 585–588, https://doi.org/10.1038/ngeo581.

King, E.L., Sejrup, H.P., Haflidason, H., Elverhøi, A. and Aarseth, I. 1996. Quaternary seismic stratigraphy of the North Sea Fan: Glaciallyfed gravity flow aprons, hemipelagic sediments, and large submarine slides. Marine Geology, 130, 293–315, https://doi.org/10.1016/0025-3227(95)00168-9.

King, L.H. 1993. Till in the marine environment. Journal of Quaternary Science, 8, 347–358, https://doi.org/10.1002/JQS.3390080406.

Kirkham, J.D., Hogan, K.A., Larter, R.D., Self, E., Games, K., Huuse, M., Stewart, M.A., Ottesen, D., Arnold, N.S. and Dowdeswell, J.A. 2021. Tunnel valley infill and genesis revealed by high-resolution 3-D seismic data. Geology, 49, 1516–1520, https://doi.org/10.1130/G49048.1.

Kleiven, H.F., Jansen, E., Fronval, T. and Smith, T.M. 2002. Intensification of Northern Hemisphere glaciations in the circum Atlantic region (3.5-2.4 Ma) - Ice-rafted detritus evidence. Palaeogeography, Palaeoclimatology, Palaeoecology, 184, 213–223, https://doi.org/10.1016/S0031-0182(01)00407-2.

Knies, J. and Gaina, C. 2008. Middle Miocene ice sheet expansion in the Arctic: Views from the Barents Sea. Geochemistry, Geophysics, Geosystems, 9, Q02015, https://doi.org/10.1029/2007GC001824.

Knies, J., Matthiessen, J., Vogt, C., Laberg, J.S., Hjelstuen, B.O., Smelror, M., Larsen, E., Andreassen, K., Eidvin, T. and Vorren, T.O. 2009. The Plio-Pleistocene glaciation of the Barents Sea-Svalbard region: a new model based on revised chronostratigraphy. Quaternary Science Reviews, 28, 812–829, https://doi.org/10.1016/j.quascirev.2008.12.002.

Knutz, P.C., Newton, A.M.W., Hopper, J.R., Huuse, M., Gregersen, U., Sheldon, E. and Dybkjær, K. 2019. Eleven phases of Greenland Ice Sheet shelf-edge advance over the past 2.7 million years. Nature Geoscience, 12, 361–368, https://doi.org/10.1038/s41561-019-0340-8.

Krissek, L.A. 1989. Late Cenozoic records of ice-rafting at ODP sites 642, 643, and 644, Norwegian Sea: onset, chronology, and characteristics of glacial/interglacial fluctuations. In: Eldholm, O., Thiede, J., Taylor, E. and Al., E. (eds) Proc. ODP. Sci. Results, 104, 61–74.

Krissek, L.A. 1995. Late Cenozoic ice-rafting records from Leg 145 sites in the North Pacific: late Miocene onset, late Pliocene intensification, and Pliocene–Pleistocene events. In: Rea, D. K., Basov, I. A., Scholl, D. W. and Allan, J. F. (eds) Proc. ODP, Sci. Results, 145. 179–194.

Kristensen, T.B., Huuse, M., Piotrowski, J.A. and Clausen, O.R. 2007. A morphometric analysis of tunnel valleys in the eastern North Sea based on 3D seismic data. Journal of Quaternary Science, 22, 801–815, https://doi.org/10.1002/jqs.1123.

Kuhlmann, G. and Wong, T.E. 2008. Pliocene paleoenvironment evolution as interpreted from 3D-seismic data in the southern North Sea, Dutch offshore sector. Marine and Petroleum Geology, 25, 173–189, https://doi.org/10.1016/j.marpetgeo.2007.05.009.

L'Heureux, J.S., Vanneste, M., Rise, L., Brendryen, J., Forsberg, C.F., Nadim, F., Longva, O., Chand, S., Kvalstad, T.J. and Haflidason, H. 2013. Stability, mobility and failure mechanism for landslides at the upper continental slope off Vesterålen, Norway. Marine Geology, 346, 192–207, https://doi.org/10.1016/J.MARGEO.2013.09.009.

Laberg, J.S. and Vorren, T.O. 1995. Late Weichselian submarine debris flow deposits on the Bear Island Trough Mouth Fan. Marine Geology, 127, 45–72, https://doi.org/10.1016/0025-3227(95)00055-4.

Laberg, J.S., Guidard, S., Mienert, J., Vorren, T.O., Haflidason, H. and Nygård, A. 2007. Morphology and morphogenesis of a high-latitude canyon; the Andøya Canyon, Norwegian Sea. Marine Geology, 246, 68–85, https://doi.org/10.1016/j.margeo.2007.01.009.

Laberg, J.S., Eilertsen, R.S. and Vorren, T.O. 2009. The paleo-ice stream in Vestfjorden, North Norway, over the last 35 k.y.: Glacial erosion and sediment yield. Bulletin of the Geological Society of America, 121, 434–447, https://doi.org/10.1130/B26277.1.

Laberg, J.S., Andreassen, K., Knies, J., Vorren, T.O. and Winsborrow, M. 2010. Late Pliocene-Pleistocene development of the Barents Sea ice sheet. Geology, 38, 107–110, https://doi.org/10.1130/G30193.1.

Laberg, J.S., Forwick, M., Husum, K. and Nielsen, T. 2013. A re-evaluation of the Pleistocene behavior of the Scoresby Sund sector of the Greenland ice sheet. Geology, 41, 1231–1234, https://doi.org/10.1130/G34784.1.

Lamb, R.M., Huuse, M. and Stewart, M. 2017. Early Quaternary sedimentary processes and palaeoenvironments in the central North Sea. Journal of Quaternary Science, 32, 127-144-undefined, https://doi.org/10.1002/jqs.2894.

Lamb, R.M., Harding, R., Huuse, M., Stewart, M. and Brocklehurst, S.H. 2018. The early quaternary North Sea basin. Journal of the Geological Society, 175, 257–290, https://doi.org/10.1144/jgs2017-057.

Larsen, H.C., Saunders, A.D., Clift, P.D., Beget, J., Wei, W., Spezzaferri, S., Ali, J., Cambray, H., Demant, A., Fitton, G., Fram, M.S., Fukuma, K., Gieskes, J., Holmes, M.A., Hunt, J., Lacasse, C., Larsen, L.M., Lykke-Andersen, H., Meltser, A., Morrison, M.L., Nemoto, N., Okay, N., Saito, S., Sinton, C., Stax, R., Vallier, T.L., Vandamme, D. and Werner, R. 1994. Seven million years of glaciation in Greenland. Science, 264, 952–955, https://doi.org/10.1126/science.264.5161.952.

Laukhun, S.A., Klimanov, V.A. and Belaya, B. V. 1999. Late Pliocene and Pleistocene palaeoclimates in Northeatern Chukotka. Sb. Geol. Antropozoikum, 23, 17–24.

LeBlanc, D.E., Shakun, J.D., Corbett, L.B., Bierman, P.R., Caffee, M.W. and Hidy, A.J. 2023. Laurentide Ice Sheet persistence during Pleistocene interglacials. Geology, 51, 496–499, https://doi.org/10.1130/G50820.1/5806814/G50820.PDF.

Lien, Ø.F., Hjelstuen, B.O., Zhang, X. and Sejrup, H.P. 2022. Late Plio-Pleistocene evolution of the Eurasian Ice Sheets inferred from sediment input along the northeastern Atlantic continental margin. Quaternary Science Reviews, 282, 107433, https://doi.org/10.1016/J.QUASCIREV.2022.107433.

Lisiecki, L.E. and Raymo, M.E. 2005. A Pliocene-Pleistocene stack of 57 globally distributed benthic δ 18O records. Paleoceanography, 20, PA1003, https://doi.org/10.1029/2004PA001071.

Lloyd, C., Huuse, M., Barrett, B.J., Stewart, M.A. and Newton, A.M.W. 2021a. A regional CO2 containment assessment of the northern Utsira Formation seal and overburden, northern North Sea. Basin Research, 33, 1985–2017, https://doi.org/10.1111/bre.12545.

Lloyd, C., Huuse, M., Barrett, B.J. and Newton, A.M.W. 2021b. Regional Exploration and Characterisation of CO2 Storage Prospects in the Utsira-Skade Aquifer, North Viking Graben, North Sea. Earth Science, Systems and Society, 1, 10041, https://doi.org/10.3389/esss.2021.10041.

Løseth, H., Dowdeswell, J.A., Batchelor, C.L. and Ottesen, D. 2020. 3D sedimentary architecture showing the inception of an Ice Age. Nature Communications, 11, 2975, https://doi.org/10.1038/s41467-020-16776-7.

Løseth, H., Nygård, A., Batchelor, C.L. and Fayzullaev, T. 2022. A regionally consistent 3D seismic-stratigraphic framework and age model for the Quaternary sediments of the northern North Sea. Marine and Petroleum Geology, 142, 105766, https://doi.org/10.1016/J.MARPETGEO.2022.105766.

Mahaney, W.C. 2004. Quaternary glacial chronology of Mount Kenya massif. Developments in Quaternary Science, 2, 227–231, https://doi.org/10.1016/S1571-0866(04)80128-3.

Maizels, J. 2002. Sediments and landforms of modern proglacial terrestrial environments. In: Menzies, J. (eds) Modern and Past Glacial Environments. Elsevier, Amsterdam, 279–316., https://doi.org/10.1016/b978-075064226-2/50012-x.

Mangerud, J., Jansen, E. and Landvik, J.Y. 1996. Late Cenozoic history of the Scandinavian and Barents Sea ice sheets. Global and Planetary Change, 12, 11–26, https://doi.org/10.1016/0921-8181(95)00009-7.

McClymont, E.L., Ho, S.L., Ford, H.L., Bailey, I., Berke, M.A., Bolton, C.T., De Schepper, S., Grant, G.R., Groeneveld, J., Inglis, G.N., Karas, C., Patterson, M.O., Swann, G.E.A., Thirumalai, K., White, S.M., Alonso-Garcia, M., Anand, P., Hoogakker, B.A.A., Littler, K., Petrick, B.F., Risebrobakken, B., Abell, J.T., Crocker, A.J., de Graaf, F., Feakins, S.J., Hargreaves, J.C., Jones, C.L., Markowska, M., Ratnayake, A.S., Stepanek, C. and Tangunan, D. 2023. Climate Evolution Through the Onset and Intensification of Northern Hemisphere Glaciation. Reviews of Geophysics, 61, e2022RG000793, https://doi.org/10.1029/2022RG000793.

Montelli, A., Dowdeswell, J.A., Ottesen, D. and Johansen, S.E. 2017. Ice-sheet dynamics through the Quaternary on the mid-Norwegian continental margin inferred from 3D seismic data. Marine and Petroleum Geology, 80, 228–242, https://doi.org/10.1016/j.marpetgeo.2016.12.002.

Montelli, A., Dowdeswell, J.A., Ottesen, D. and Johansen, S.E. 2018a. 3D seismic evidence of buried iceberg ploughmarks from the mid-Norwegian continental margin reveals largely persistent North Atlantic Current through the Quaternary. Marine Geology, 399, 66–83, https://doi.org/10.1016/j.margeo.2017.11.016.

Montelli, A., Dowdeswell, J.A., Ottesen, D. and Johansen, S.E. 2018b. Architecture and sedimentary processes on the mid-Norwegian continental slope: A 2.7 Myr record from extensive seismic evidence. Quaternary Science Reviews, 192, 185–207, https://doi.org/10.1016/j.quascirev.2018.05.034.

Montelli, A., Gulick, S.P.S., Fernandez, R., Frederick, B.C., Shevenell, A.E., Leventer, A. and Blankenship, D.D. 2019. Seismic stratigraphy of the Sabrina Coast shelf, East Antarctica: Early history of dynamic meltwater-rich glaciations. GSA Bulletin, 132, 545–561, https://doi.org/10.1130/b35100.1.

Montelli, A., Dowdeswell, J.A., Pirogova, A., Terekhina, Y., Tokarev, M., Rybin, N., Martyn, A. and Khoshtariya, V. 2020. Deep and extensive meltwater system beneath the former Eurasian Ice Sheet in the Kara Sea. Geology, 48, 179–183, https://doi.org/10.1130/G46968.1.

Moreau, J., Huuse, M., Janszen, A., Vegt, V. Der, Gibbard, P.L. and Moscariello, A. 2012. The glaciogenic unconformity of the southern North Sea. In: Huuse, M., Redfern, J., Le Heron, D. P., Dixon, R. J., Moscariello, A. and Craig, J. (eds) Glaciogenic Reservoirs and Hydrocarbon Systems. Geological Society, London, Special Publication, 368, 99–110., https://doi.org/10.1144/SP368.5.

Muttoni, G., Carcano, C., Garzanti, E., Ghielmi, M., Piccin, A., Pini, R., Rogledi, S. and Sciunnach, D. 2003. Onset of major Pleistocene glaciations in the Alps. Geology, 31, 989–992, https://doi.org/10.1130/G19445.1.

Newnham, R.M., Lowe, D.J. and Williams, P.W. 2016. Quaternary environmental change in New Zealand: a review. http://dx.doi.org/10.1177/030913339902300406, 23, 567–610, https://doi.org/10.1177/030913339902300406.

Newton, A.M., Huuse, M., Knutz, P. and Cox, D. 2020. Repeated ice streaming on the northwest Greenland shelf since the onset of the Middle Pleistocene Transition. The Cryosphere, 14, 2303–2312, https://doi.org/10.5194/tc-2019-268.

Newton, A.M.W. 2017. Seismic Geomorphology of Glaciated Margins. University of Manchester, PhD Thesis.

Newton, A.M.W. and Huuse, M. 2017a. Glacial geomorphology of the central Barents Sea: Implications for the dynamic deglaciation of the Barents Sea Ice Sheet. Marine Geology, 387, 114–131, https://doi.org/10.1016/j.margeo.2017.04.001.

Newton, A.M.W. and Huuse, M. 2017b. Late Cenozoic environmental changes along the Norwegian margin. Marine Geology, 393, 216–244, https://doi.org/10.1016/j.margeo.2017.05.004.

Newton, A.M.W., Huuse, M. and Brocklehurst, S.H. 2016. Buried iceberg scours reveal reduced North Atlantic Current during the stage 12 deglacial. Nature Communications, 7, 10927, https://doi.org/10.1038/ncomms10927.

Newton, A.M.W., Huuse, M. and Brocklehurst, S.H. 2018. A Persistent Norwegian Atlantic Current Through the Pleistocene Glacials. Geophysical Research Letters, 45, 5599–5608, https://doi.org/10.1029/2018GL077819.

Newton, A.M.W., Huuse, M., Cox, D.R. and Knutz, P.C. 2021. Seismic geomorphology and evolution of the Melville Bugt trough mouth fan, northwest Greenland. Quaternary Science Reviews, 255, https://doi.org/10.1016/j.quascirev.2021.106798.

Nielsen, T. and Kuijpers, A. 2013. Only 5 southern Greenland shelf edge glaciations since the early Pliocene. Scientific Reports, 3, 1875, https://doi.org/10.1038/srep01875.

Nielsen, T., De Santis, L., Dahlgren, K.I.T., Kuijpers, A., Laberg, J.S., Nygård, A., Praeg, D. and Stoker, M.S. 2005. A comparison of the NW European glaciated margin with other glaciated margins. Marine and Petroleum Geology, 22, 1149–1183, https://doi.org/10.1016/j.marpetgeo.2004.12.007.

Nielsen, T., Mathiesen, A. and Bryde-Auken, M. 2007. Base quaternary in the Danish parts of the North Sea and Skagerrak. Geological Survey of Denmark and Greenland Bulletin, 15, 37–40.

Nygård, A., Sejrup, H.P., Haflidason, H. and Bryn, P. 2005. The glacial North Sea Fan, southern Norwegian Margin: Architecture and evolution from the upper continental slope to the deep-sea basin. Marine and Petroleum Geology, 22, 71–84, https://doi.org/10.1016/j.marpetgeo.2004.12.001.

Ó Cofaigh, C. 1996. Tunnel valley genesis. Progress in Physical Geography, 20, 1–19, https://doi.org/10.1177/030913339602000101.

Ó Cofaigh, C., Taylor, J., Dowdeswell, J.A. and Pudsey, C.J. 2003. Palaeo-ice streams, trough mouth fans and high-latitude continental slope sedimentation. Boreas, 32, 37–55, https://doi.org/10.1080/03009480310001858.

Ottesen, D., Dowdeswell, J.A. and Rise, L. 2005a. Submarine landforms and the reconstruction of fast-flowing ice streams within a large Quaternary ice sheet: The 2500-km-long Norwegian-Svalbard margin (57°-80°N). Bulletin of the Geological Society of America, 117, 1033–1050, https://doi.org/10.1130/B25577.1.

Ottesen, D., Rise, L., Knies, J., Olsen, L. and Henriksen, S. 2005b. The Vestfjorden-Trænadjupet palaeo-ice stream drainage system, mid-Norwegian continental shelf. Marine Geology, 218, 175–189, https://doi.org/10.1016/j.margeo.2005.03.001.

Ottesen, D., Stokes, C.R., Rise, L. and Olsen, L. 2008. Ice-sheet dynamics and ice streaming along the coastal parts of northern Norway. Quaternary Science Reviews, 27, 922–940, https://doi.org/10.1016/j.quascirev.2008.01.014.

Ottesen, D., Rise, L., Andersen, E.S., Bugge, T. and Eidvin, T. 2009. Geological evolution of the norwegian continental shelf between 61°N and 68°N during the last 3 million years. Norsk Geologisk Tidsskrift, 89, 251–265.

Ottesen, D., Dowdeswell, J.A., Rise, L. and Bugge, T. 2012. Large-scale development of the mid-Norwegian shelf over the last three million years and potential for hydrocarbon reservoirs in glacial sediments. In: Huuse, M., Redfern, J., Le Heron, D. P., Dixon, R. J., Moscariello, A. and Craig, J. (eds) Glaciogenic Reservoirs and Hydrocarbon Systems. Geological Society, London, Special Publication, 368, 53–73., https://doi.org/10.1144/sp368.6.

Ottesen, D., Dowdeswell, J.A. and Bugge, T. 2014. Morphology, sedimentary infill and depositional environments of the Early Quaternary North Sea Basin (56°-62°N). Marine and Petroleum Geology, 56, 123–146, https://doi.org/10.1016/j.marpetgeo.2014.04.007.

Ottesen, D., Stokes, C.R., Bøe, R., Rise, L., Longva, O., Thorsnes, T., Olesen, O., Bugge, T., Lepland, A. and Hestvik, O.B. 2016a. Landform assemblages and sedimentary processes along the Norwegian Channel Ice Stream. Sedimentary Geology, 338, 115–137, https://doi.org/10.1016/j.sedgeo.2016.01.024.

Ottesen, D., Dowdeswell, J.A., Rise, L., Thorsnes, T. and Bellec, V.K. 2016b. Lateral ice-stream shear-margin moraines on north Norwegian shelves. In: Dowdeswell, J. A., Canals, M., Jakobsson, M., Todd, B. J., Dowdeswell, E. K. and Hogan, K. A. (eds) Atlas of Submarine Glacial Landforms: Modern, Quaternary and Ancient. Geological Society, London, Memoir, 46, 191–192., https://doi.org/10.1144/M46.134.

Ottesen, D., Batchelor, C.L., Dowdeswell, J.A. and Løseth, H. 2018. Morphology and pattern of Quaternary sedimentation in the North Sea Basin (52–62°N). Marine and Petroleum Geology, 98, 836–859, https://doi.org/10.1016/j.marpetgeo.2018.08.022.

Ottesen, D., Stewart, M., Brönner, M. and Batchelor, C.L. 2020. Tunnel valleys of the central and northern North Sea (56°N to 62°N): Distribution and characteristics. Marine Geology, 425, 106199, https://doi.org/10.1016/j.margeo.2020.106199.

Pérez, L.F., Nielsen, T., Knutz, P.C., Kuijpers, A. and Damm, V. 2018. Large-scale evolution of the central-east Greenland margin: New insights to the North Atlantic glaciation history. Global and Planetary Change, 163, 141–157, https://doi.org/10.1016/j.gloplacha.2017.12.010.

Phillips, E., Hodgson, D.M. and Emery, A.R. 2017. The Quaternary geology of the North Sea basin. Journal of Quaternary Science, 32, 117–126, https://doi.org/10.1002/JQS.2932.

Piasecka, E.D., Winsborrow, M.C.M., Andreassen, K. and Stokes, C.R. 2016. Reconstructing the retreat dynamics of the Bjørnøyrenna Ice Stream based on new 3D seismic data from the central Barents Sea. Quaternary Science Reviews, 151, 212–227, https://doi.org/10.1016/j.quascirev.2016.09.003.

Piotrowski, J.A. 1994. Tunnel-valley formation in northwest Germany—geology, mechanisms of formation and subglacial bed conditions for the Bornhöved tunnel valley. Sedimentary Geology, 89, 107–141, https://doi.org/10.1016/0037-0738(94)90086-8.

Posamentier, H.W. 2004. Seismic Geomorphology: Imaging Elements of Depositional Systems from Shelf to Deep Basin Using 3D Seismic Data: Implications for Exploration and Development. In: Davies, R. J., Cartwright, J. A., Stewart, S. A., Lappin, M. and Underhill, J. R. (eds) 3D Seismic Technology: Application to the Exploration of Sedimentary Basins. Geological Society, London, Memoir, 29, 11–24., https://doi.org/10.1144/GSL.MEM.2004.029.01.02.

Posamentier, H.W., Davies, R.J., Cartwright, J.A. and Wood, L. 2007. Seismic geomorphology - an overview. In: Davies, R. J., Posamentier, H. W., Wood, L. and Cartwright, J. A. (eds) Seismic Geomorphology: Applications to Hydrocarbon Exploration and Production. Geological Society, London, Special Publication 277 1–14., https://doi.org/10.1144/gsl.sp.2007.277.01.01.

Posamentier, H.W., Paumard, V. and Lang, S.C. 2022. Principles of seismic stratigraphy and seismic geomorphology I: Extracting geologic insights from seismic data. Earth-Science Reviews, 228, 103963, https://doi.org/10.1016/J.EARSCIREV.2022.103963.

Praeg, D. 2003. Seismic imaging of mid-Pleistocene tunnel-valleys in the North Sea Basin-high resolution from low frequencies. Journal of Applied Geophysics, 53, 273–298, https://doi.org/10.1016/j.jappgeo.2003.08.001.

Preusser, F., Graf, H.R. and Schlüchter, C. 2011. Quaternary glaciation history of northern switzerland. Quaternary Science Journal, 60, 282–305, https://doi.org/10.3285/eg.60.2-3.06.

Rabassa, J. 2008. Late Cenozoic Glaciations in Patagonia and Tierra del Fuego. Developments in Quaternary Science, 11, 151–204, https://doi.org/10.1016/S1571-0866(07)10008-7.

Rea, B.R., Newton, A.M.W., Lamb, R.M., Harding, R., Bigg, G.R., Rose, P., Spagnolo, M., Huuse, M., Cater, J.M.L., Archer, S., Buckley, F., Halliyeva, M., Huuse, J., Cornwell, D.G., Brocklehurst, S.H. and Howell, J.A. 2018. Extensive marine-terminating ice sheets in Europe from 2.5 million years ago. Science Advances, 4, eaar8327, https://doi.org/10.1126/sciadv.aar8327.

Reinardy, B.T.I., Sejrup, H.P., Hjelstuen, B.O., King, E. and Augedal, H. 2018. A Quaternary aminostratigraphy constraining chronology of depositional environments in the North Sea Basin. Marine Geology, 402, 139–152, https://doi.org/10.1016/j.margeo.2017.11.004.

Rise, L., Olesen, O., Rokoengen, K., Ottesen, D. and Riis, F. 2004. Mid-Pleistocene ice drainage pattern in the Norwegian Channel imaged by 3D seismic. Quaternary Science Reviews, 23, 2323–2335, https://doi.org/10.1016/j.quascirev.2004.04.005.

Rise, L., Ottesen, D., Berg, K. and Lundin, E. 2005. Large-scale development of the mid-Norwegian margin during the last 3 million years. Marine and Petroleum Geology, 22, 33–44, https://doi.org/10.1016/j.marpetgeo.2004.10.010.

Rise, L., Chand, S., Hjelstuen, B.O., Haflidason, H. and Bøe, R. 2010. Late Cenozoic geological development of the south Vøring margin, mid-Norway. Marine and Petroleum Geology, 27, 1789–1803, https://doi.org/10.1016/j.marpetgeo.2010.09.001.

Rise, L., Bøe, R., Riis, F., Bellec, V.K., Laberg, J.S., Eidvin, T., Elvenes, S. and Thorsnes, T. 2013. The Lofoten-Vesterålen continental margin, North Norway: Canyons and mass-movement activity. Marine and Petroleum Geology, 45, 134–149, https://doi.org/10.1016/j.marpetgeo.2013.04.021.

Rise, L., Bellec, V.K., Ottesen, D., Bøe, R. and Thorsnes, T. 2016. Hill-hole pairs on the Norwegian continental shelf. In: Dowdeswell, J. A., Canals, M., Jakobsson, M., Todd, B. J., Dowdeswell, E. K. and Hogan, K. A. (eds) Atlas of Submarine Glacial Landforms: Modern, Quaternary and Ancient. Geological Society, London, Memoir, 46, 203–204., https://doi.org/10.1144/M46.42.

Rose, P., Byerley, G., Vaughan, O., Cater, J., Rea, B.R., Spagnolo, M. and Archer, S. 2018. Aviat: A Lower Pleistocene shallow gas hazard developed as a fuel gas supply for the Forties Field. Petroleum Geology Conference Proceedings, 8, 485–505, https://doi.org/10.1144/PGC8.16.

Rundberg, Y. and Eidvin, T. 2005. Controls on depositional history and architecture of the Oligocene-Miocene succession, northern North Sea Basin. In: Wandås, B., Nystuen, J. P., Eide, E. A. and Gradstein, F. M. (eds) Onshore-Offshore Relationships on the North Atlantic Margin. Norwegian Petroleum Society, Trondheim, Special Publication, 12, 207–239., https://doi.org/10.1016/S0928-8937(05)80050-5.

Rydningen, T.A., Vorren, T.O., Laberg, J.S. and Kolstad, V. 2013. The marine-based NW Fennoscandian ice sheet: Glacial and deglacial dynamics as reconstructed from submarine landforms. Quaternary Science Reviews, 68, 126–141, https://doi.org/10.1016/j.quascirev.2013.02.013.

Rydningen, T.A., Laberg, J.S. and Kolstad, V. 2016. Late Cenozoic evolution of high-gradient trough mouth fans and canyons on the glaciated continental margin offshore Troms, northern Norway-Paleoclimatic implications and sediment yield. Bulletin of the Geological Society of America, 128, 576–596, https://doi.org/10.1130/B31302.1.

Schaefer, J.M., Finkel, R.C., Balco, G., Alley, R.B., Caffee, M.W., Briner, J.P., Young, N.E., Gow, A.J. and Schwartz, R. 2016. Greenland was nearly ice-free for extended periods during the Pleistocene. Nature, 540, 252–255, https://doi.org/10.1038/nature20146.

Sejrup, H.P., Aarseth, I., Haflidason, H., Løvlie, R., Bratten, Å., Tjøstheim, G., Forsberg, C.F. and Ellingsen, K.L. 1995. Quaternary of the Norwegian Channel: glaciation history and palaeoceanography. Norsk Geologisk Tidsskrift, 75, 65–87.

Sejrup, H.P., Larsen, E., Landvik, J., King, E.L., Haflidason, H. and Nesje, A. 2000. Quaternary glaciations in southern Fennoscandia: Evidence from southwestern Norway and the northern North Sea region. Quaternary Science Reviews, 19, 667–685, https://doi.org/10.1016/S0277-3791(99)00016-5.

Sejrup, H.P., Larsen, E., Haflidason, H., Berstad, I.M., Hjelstuen, B.O., Jonsdottir, H.E., L. King, E.L., Landvik, J., Longva, O., Nygård, A., Ottesen, D., Raunholm, S., Rise, L. and Stalsberg, K. 2003. Configuration, history and impact of the Norwegian Channel Ice Stream. Boreas, 32, 18–36, https://doi.org/10.1080/03009480310001029.

Sejrup, H.P., Clark, C.D. and Hjelstuen, B.O. 2016. Rapid ice sheet retreat triggered by ice stream debuttressing: Evidence from the North Sea. Geology, 44, 355–358, https://doi.org/10.1130/G37652.1.

Shakun, J.D., Raymo, M.E. and Lea, D.W. 2016. An early Pleistocene Mg/Ca-δ^{18}O record from the Gulf of Mexico: Evaluating ice sheet size and pacing in the 41-kyr world. Paleoceanography, 31, 1011–1027, https://doi.org/10.1002/2016PA002956.

Smith, R.T. and Anderson, J.B. 2010. Ice-sheet evolution in James Ross Basin, Weddell Sea margin of the Antarctic Peninsula: The seismic stratigraphic record. GSA Bulletin, 122, 830–842, https://doi.org/10.1130/B26486.1.

Solgaard, A.M., Reeh, N., Japsen, P. and Nielsen, T. 2011. Snapshots of the Greenland ice sheet configuration in the Pliocene to early Pleistocene. Journal of Glaciology, 57, 871–880, https://doi.org/10.3189/002214311798043816.

Spagnolo, M., Clark, C.D., Ely, J.C., Stokes, C.R., Anderson, J.B., Andreassen, K., Graham, A.G.C. and King, E.C. 2014. Size, shape and spatial arrangement of mega-scale glacial lineations from a large and diverse dataset. Earth Surface Processes and Landforms, 39, 1432–1448, https://doi.org/10.1002/esp.3532.

Spagnolo, M., Phillips, E., Piotrowski, J.A., Rea, B.R., Clark, C.D., Stokes, C.R., Carr, S.J., Ely, J.C., Ribolini, A., Wysota, W. and Szuman, I. 2016. Ice stream motion facilitated by a shallow-deforming and accreting bed. Nature Communications, 7, 10723, https://doi.org/10.1038/ncomms10723.

Spratt, R.M. and Lisiecki, L.E. 2016. A Late Pleistocene sea level stack. Climate of the Past, 12, 1079–1092, https://doi.org/10.5194/CP-12-1079-2016.

Stewart, M.A. and Lonergan, L. 2011. Seven glacial cycles in the middle-late Pleistocene of northwest Europe: Geomorphic evidence from buried tunnel valleys. Geology, 39, 283–286, https://doi.org/10.1130/G31631.1.

Stroeven, A.P., Hättestrand, C., Kleman, J., Heyman, J., Fabel, D., Fredin, O., Goodfellow, B.W., Harbor, J.M., Jansen, J.D., Olsen, L., Caffee, M.W., Fink, D., Lundqvist, J., Rosqvist, G.C., Strömberg, B. and Jansson, K.N. 2016. Deglaciation of Fennoscandia. Quaternary Science Reviews, 147, 91–121, https://doi.org/10.1016/j.quascirev.2015.09.016.

Suggate, R.P. 1990. Late pliocene and quaternary glaciations of New Zealand. Quaternary Science Reviews, 9, 175–197, https://doi.org/10.1016/0277-3791(90)90017-5.

Taylor, J., Dowdeswell, J.A., Kenyon, N.H. and Ó Cofaigh, C. 2002. Late Quaternary architecture of trough-mouth fans: debris flows and suspended sediments on the Norwegian margin. In: Dowdeswell, J.A. and Ó Cofaigh, C. (eds) Glacier-Influenced Sedimentation on High-Latitude Continental Margin. Geological Society, London, Special Publication, 203, 55–71., https://doi.org/10.1144/gsl.sp.2002.203.01.04.

Thierens, M., Pirlet, H., Colin, C., Latruwe, K., Vanhaecke, F., Lee, J.R., Stuut, J.-B., Titschack, J., Huvenne, V.A.I., Dorschel, B., Wheeler, A.J. and Henriet, J.-P. 2012. Ice-rafting from the British-Irish ice sheet since the earliest Pleistocene (2.6 million years ago): Implications for long-term mid-latitudinal ice-sheet growth in the North Atlantic region. Quaternary Science Reviews, 44, 229–240, https://doi.org/10.1016/j.quascirev.2010.12.020.

Thöle, H., Gaedicke, C., Kuhlmann, G. and Reinhardt, L. 2014. Late Cenozoic sedimentary evolution of the German North Sea - A seismic stratigraphic approach. Newsletters on Stratigraphy, 47/3, 299–329, https://doi.org/10.1127/0078-0421/2014/0049.

Todd, B.J., Lewis, C.F.M. and Ryall, P.J.C. 1988. Comparison of trends of iceberg scour marks with iceberg trajectories and evidence of paleocurrent trends on Saglek Bank, northern Labrador Shelf. Canadian Journal of Earth Sciences, 25, 1374–1383, https://doi.org/10.1139/e88-132.

Van Der Vegt, P., Janszen, A. and Moscariello, A. 2012. Tunnel valleys: Current knowledge and future perspectives. In: Huuse, M., Redfern, J., Le Heron, D. P., Dixon, R. J., Moscariello, A. and Craig, J. (eds) Glaciogenic Reservoirs and Hydrocarbon Systems. Geological Society, London, Special Publication, 368, 75–97., https://doi.org/10.1144/SP368.13.

Waage, M., Bünz, S., Bøe, R. and Mienert, J. 2018. High-resolution 3D seismic exhibits new insights into the middle-late Pleistocene stratigraphic evolution and sedimentary processes of the Bear Island trough mouth fan. Marine Geology, 403, 139–149, https://doi.org/10.1016/j.margeo.2018.05.006.

Willeit, M., Ganopolski, A., Calov, R. and Brovkin, V. 2019. Mid-Pleistocene transition in glacial cycles explained by declining CO_2 and regolith removal. Science Advances, 5, eaav7337, https://doi.org/10.1126/sciadv.aav7337.

Winsborrow, M., Andreassen, K., Hubbard, A., Plaza-Faverola, A., Gudlaugsson, E. and Patton, H. 2016. Regulation of ice stream flow through subglacial formation of gas hydrates. Nature Geoscience, 9, 370–374, https://doi.org/10.1038/ngeo2696.

Winsborrow, M.C.M., Andreassen, K., Corner, G.D. and Laberg, J.S. 2010. Deglaciation of a marine-based ice sheet: Late Weichselian palaeo-ice dynamics and retreat in the southern Barents Sea reconstructed from onshore and offshore glacial geomorphology. Quaternary Science Reviews, 29, 424–442, https://doi.org/10.1016/j.quascirev.2009.10.001.

Woodworth-Lynas, C.M.T., Simms, A. and Rendell, C.M. 1985. Iceberg grounding and scouring on the Labrador Continental Shelf. Cold Regions Science and Technology, 10, 163–186, https://doi.org/10.1016/0165-232X(85)90028-X.

Figure Captions

Figure 1: Study site area – (**a**) Bathymetric map of northwest Europe. Locations of seismic profiles and maps in subsequent figures are shown. Bathymetry data from EMODnet Bathymetry Consortium (EMODnet Bathymetry Consortium 2018) and satellite imagery the World Imagery layer on ArcMap Online. Note the non-linear colour scale to accentuate contemporary shelf morphology. (**b**) A simplified isopach map showing the thickness of the glacigenic succession along the margin. This has been compiled from several published maps manually stitched together (Ottesen *et al.* 2012, 2014, 2018; Rydningen *et al.* 2016; Lamb *et al.* 2018; Rea *et al.* 2018). Maps in the time domain have been depth converted using a P-wave velocity of 1800 m s^{-1}. (**c**) Distribution of the 3D seismic data used in this study shown in yellow – note that 2D line coverage is largely basin-wide and has been left off for clarity. Red circles are boreholes mentioned in the text. Key place names in the text are shown. Abbreviations are as follows: Andøya Canyon (AC), Barents Sea (BS), Bjørnøyrenna Trough Mouth Fan (BTMF), Central North Sea (CNS), Lofoten (L), Måløy Plateau (MP), Mid-Norwegian Margin (MNM), Møre Basin (MB), Norwegian Channel (NC), Northern North Sea (NNS), North Sea Fan (NSF), Southern North Sea (SNS), Troms (T), Vøring Plateau (VP).

Figure 2: Glacial stratigraphy – cartoons showing the seismic stratigraphy of: (**a**) southwest Barents Sea, (**b**) Troms, offshore northern Norway, (**c**) mid-Norwegian margin, (**d**) northern North Sea, (**e**) central North Sea, (**f**) southern North Sea. (**g**) Compilation of the different stratigraphic schemes, their assumed dates, and the context of the global oxygen isotope curve from Lisiecki and Raymo (2005). Grey bands indicate periods of glaciation. References for the different seismic stratigraphic schemes are shown on the panel (g).

Figure 3: Mega-scale glaciation lineations – (**a**) example of multiple sets of mega-scale glacial lineations (MSGL) atop the Barents Sea Upper Regional Unconformity. Modified after Bellwald *et al.* (2019). (**b**) MSGL surface buried within Naust N of the mid-Norwegian margin. (**c**) 3D image of MSGL buried within Naust T. The location of images in panels (e) and (f) is shown. (**d**) MSGL observed at the base of Naust A. (**e**) Dip illumination extraction on the surface shown in (c) to highlight a different imaging technique. (**f**) Curvature extraction on the surface shown in (c) to highlight a different imaging technique. (**g**) Two sets of MSGL observed on an RMS amplitude extraction on a surface buried within the middle of Naust A. (**h**) Variance timeslice at 700 ms depth showing MSGL buried within Unit D of the northern North Sea.

Figure 4: Deformation landforms – (**a**) Example of a buried hill-hole pair on the Barents Sea upper regional unconformity. Modified after Bellwald *et al.* (2023). (**b**) Buried surface within Naust T on the

mid-Norwegian margin showing a buried hill-hole pair. Note the presence of mega-scale glaciations indicating ice flow direction. Locations of panels (c) and (d) are shown. (**c**) North-south reflection seismic profile through the hole feature displayed on panel (b). (**d**) West-East seismic profile showing the hole and subsequent hill that are displayed in panel (b). (**e**) Uninterpreted seismic line showing a glacitectonic thrust complex from the central Barents Sea. Modified from Bendixen *et al*. (2018). (**f**) Interpreted version of panel (e). This shows the décollement surface, deformation and thrusting of the stratigraphy above it, and an erosional surface that is associated with subsequent tunnel valley erosion.

Figure 5: Ridge structures – (**a**) Example of regularly-spaced retreat moraines that are observed on the contemporary seafloor. (**b**) Buried transverse ridges within Naust U on the mid-Norwegian margin. These are interpreted as retreat moraines. The rhombohedral ridges may represent the only documented example of buried crevasse-squeeze ridges on the entire margin. (**c**) Buried surface within Naust S showing transverse ridges interpreted as moraines. Note the adjacent observation of mega-scale glacial lineations. (**d**) Seismic profile on the outer mid-Norwegian shelf showing the Skjoldryggen terminal moraine associated with the last glacial maximum. Note, such is the size of the moraine that some of the internal stratigraphy can be resolved with industry reflection seismic data. The dotted yellow line is the base of Naust T. (**e**) An example of a buried grounding-zone wedge (GZW) atop a glacial unconformity located within Naust U. Naust units indicated by the dotted line. (**f**) Seismic profile showing the Peon gas discovery in the northern North Sea along with the seismic horizons where other glacial landforms have been documented. Black bar shows the location of the well log in (g). Image reworked from Bellwald *et al*. (2022). (**g**) Borehole logging of Well 35/2-1 through the Peon discovery. Note the significant drop in density and velocity in the reservoir sediments. Image reworked from Bellwald *et al*. (2022).

Figure 6: Meltwater landforms – (**a**) Example of a braided river system observed on the Upper Regional Unconformity of the Barents Sea. The river system is associated with an outburst flood (Bellwald *et al.* 2021). (**b**) Undulating incision within Naust T on the mid-Norwegian margin that is interpreted as a tunnel valley. Displayed as a timeslice at -536 ms depth from a variance volume. (**c**) A river channel incised into the base of the glacial succession in the northern North Sea. The channel is associated with increased meltwater discharge from local mountain glaciers. Figure modified from Løseth *et al.* (2020). (**d**) Tunnel valley observed within Naust S on the mid-Norwegian margin. Note the mega-scale glacial lineations indicating the direction of ice flow to the southwest. (**e**) Tunnel valley observed within Naust T on the mid-Norwegian margin. Mega-scale glacial lineations indicate that ice flow was toward the northwest. (**f**) Short, relatively straight channels that terminate at small

depositional fans. These are observed on the downstream side of a grounding-zone wedge and are interpreted as proglacial channels buried in Naust T. (**g** and **h**) An uninterpreted and interpreted reflection seismic profile from the central North Sea that shows a number of cross-cutting incisional features that are interpreted as the multi-phase cutting of subglacial tunnel valleys.

Figure 7: Iceberg scours – (**a**) RMS amplitude extracted across an upper palaeo-slope surface buried within Naust N on the mid-Norwegian margin. This shows evidence of a double-keeled iceberg and an iceberg being moved by geostrophic and tidal currents (e.g., Newton *et al.* 2016). (**b**) RMS amplitude extraction across a buried surface within Unit D in the northern North Sea. (**c**) RMS amplitude extraction of a buried surface in the central North Sea that dates to ~1.95 Ma. Location of seismic line displayed in panel (d) is indicated. (**d**) Cross-section seismic profile through an iceberg scour displaying the erosional trough and adjacent depositional berms.

Figure 8: Slope features – (**a**) Minimum amplitude extraction from the North Sea Fan showing the presence of a Late Pleistocene channel-levee system associated with glacial meltwaters. Figure modified from Bellwald *et al*. (2020). (**b**) RMS amplitude extraction from a surface buried within Naust A. This shows debris flows that have been interpreted as glacigenic debris flows (GDFs). (**c**) Variance extraction timeslice at 1000 ms depth, showing an example of GDFs within Unit D in the northern North Sea.

Figure 9: Landform distribution – stratigraphic chart showing the abundance of glacial landforms documented in the different glacigenic units of the northwest European glaciated margin (Fig. 2). While there is considerable documentation of glacial landforms in the youngest units, the older units also demonstrate an abundance and variety, showing that ice cover, regardless of precise size and dynamics, have been influencing continental shelf sedimentary processes since the late Pliocene. Ice-rafted detritus (IRD) data from ODP Sites 642-644 on the mid-Norwegian margin (Jansen *et al.* 1989; Krissek 1989; Henrich and Baumann 1994) and oxygen isotope data (Lisiecki and Raymo 2005) provide context for regional and global evidence of ice sheet activity. The dashed blue line shows the southern North Sea unconformity (see Moreau et al. (2012)). Abbreviations are: crevasse-squeeze ridge (CSR), grounding-zone wedge (GZW), mega-scale glacial lineation (MSGL), and Marine Isotope Stage (MIS). Note that some units have hiatuses in which sediment does not accumulate. Given the uncertainties in timing of the hiatuses, and the desire for clarity on the figure, these have not been indicated – e.g., periods of hiatus in the earliest Pleistocene part of Clinoform Unit 1 in the Central North Sea (Fig. 2).

Table Caption

Table 1: Landform observations – table showing the most common landforms observed along the European glaciated margin and what they tell us about environmental processes. Examples displayed in figures are also indicated.

	LANDFORM	SIGNIFICANCE	FIGURE
SUBGLACIAL	Mega-scale glacial lineation	Location and direction of fast-flowing ice	3a-3h
	Hill-hole air	Evidence of glacitectonism and frozen bed conditions	4a-4d
	Crevasse-squeeze ridge	Infill of basal crevasses and ice margin stagnation	5b
	Tunnel valley	Channelised and over-pressured subglacial meltwater	6b, 6d-6e, 6g-6h
ICE-MARGINAL	Moraine	Ice margin locations at its maximum and during retreat	5a-5d
	Thrust structure	Tectonic deformation of frozen ground in front of the ice	4e-4f
	Grounding-zone wedge	Evidence of temporary stability at the ice sheet grounding-line	5e-5g
	Ice-proximal fan	Accumulation of material delivered by meltwater to the ice sheet margin	6f
PROGLACIAL	Iceberg scour	Deformation and erosion of the seafloor from grounded icebergs	7a-7d
	Proglacial channel	Fluvial channel adjacent to the ice sheet margin	6a, 6c, 6f
	Channel-gully complex	Downslope channelisation of density-driven currents	8a
	Glacigenic debris flow	Remobilisation of subglacial materials deposited at the shelf edge	8b-8c

Table 1

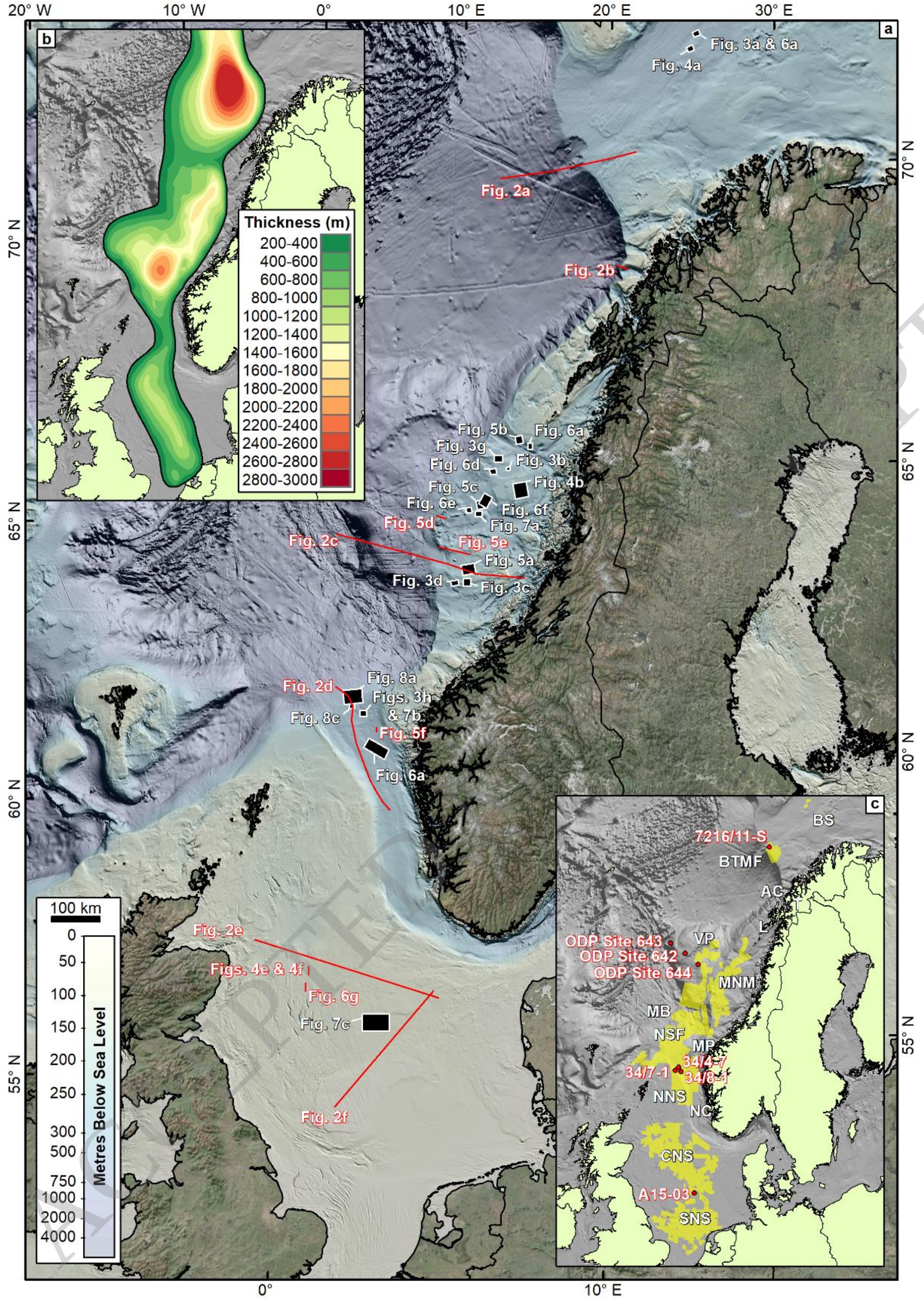
20° W
10° W
0°
10° E
20° E
30° E
70° N
65° N
60° N
55° N
a
b
c
Thickness (m)
200-400
400-600
600-800
800-1000
1000-1200
1200-1400
1400-1600
1600-1800
1800-2000
2000-2200
2200-2400
2400-2600
2600-2800
2800-3000
Fig. 3a & 6a
Fig. 4a
Fig. 2a
Fig. 2b
Fig. 5b
Fig. 6a
Fig. 3g
Fig. 6d
Fig. 3b
Fig. 5c
Fig. 4b
Fig. 6e
Fig. 6f
Fig. 5d
Fig. 7a
Fig. 2c
Fig. 5e
Fig. 5a
Fig. 3d
Fig. 3c
Fig. 2d
Fig. 8a
Figs. 3h & 7b
Fig. 8c
Fig. 5f
Fig. 6a
100 km
Metres Below Sea Level
0
50
100
150
200
250
300
500
750
1000
2000
4000
Fig. 2e
Figs. 4e & 4f
Fig. 6g
Fig. 7c
Fig. 2f
7216/11-S
BS
BTMF
AC
L
ODP Site 643
ODP Site 642
ODP Site 644
VP
MNM
MB
NSF
MP
34/4-7
34/7-1
34/8-1
NNS
NC
CNS
A15-03
SNS

Figure 1

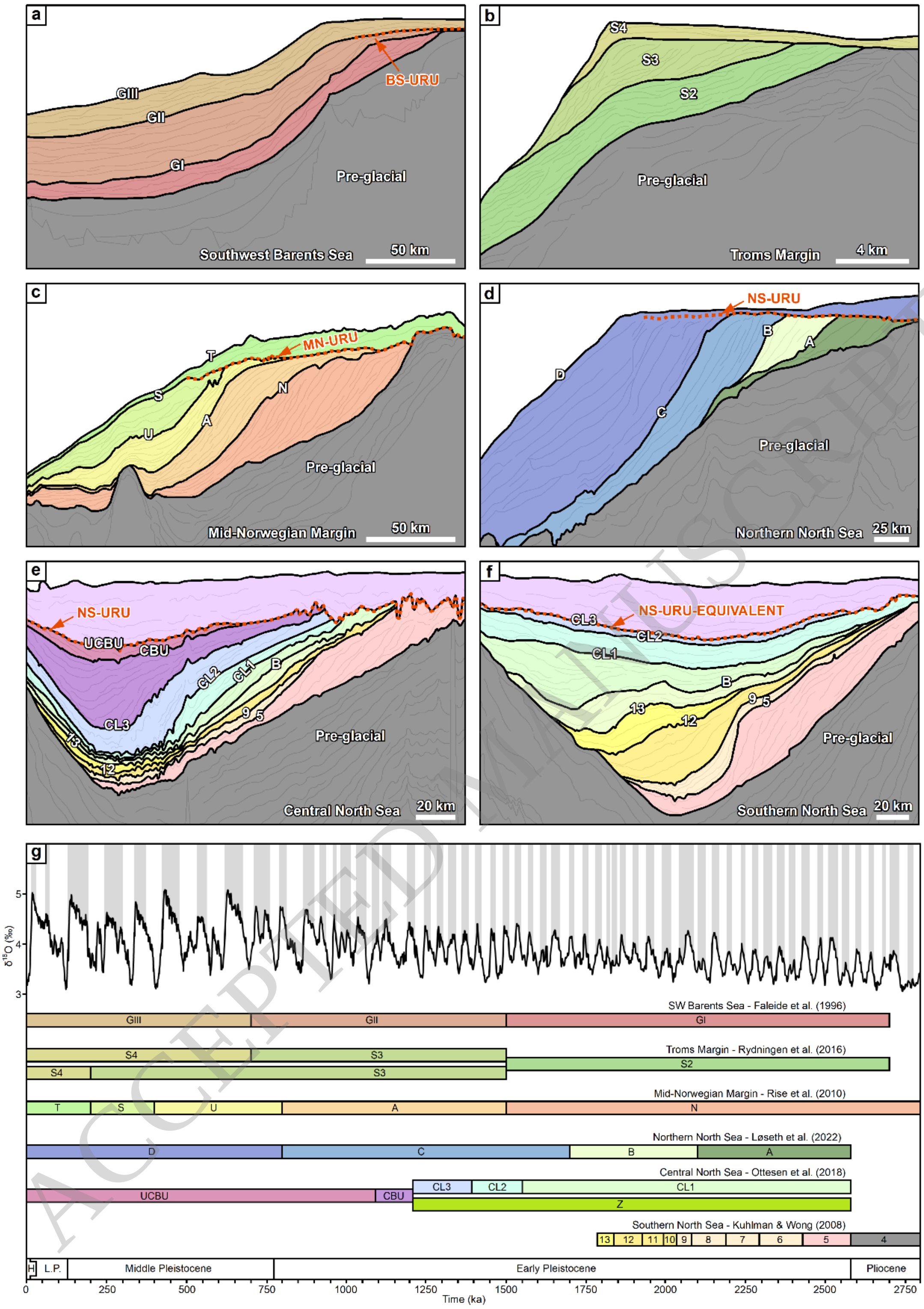

a
GIII
GII
GI
BS-URU
Pre-glacial
Southwest Barents Sea
50 km
b
S4
S3
S2
Pre-glacial
Troms Margin
4 km
c
MN-URU
T
S
U
A
N
Pre-glacial
Mid-Norwegian Margin
50 km
d
NS-URU
D
C
B
A
Pre-glacial
Northern North Sea
25 km
e
NS-URU
UCBU
CBU
CL3
CL2
CL1
B
9
5
13
12
Pre-glacial
Central North Sea
20 km
f
NS-URU-EQUIVALENT
CL3
CL2
CL1
B
9
5
13
12
Pre-glacial
Southern North Sea
20 km
g
δ18O (‰)
SW Barents Sea - Faleide et al. (1996)
Troms Margin - Rydningen et al. (2016)
Mid-Norwegian Margin - Rise et al. (2010)
Northern North Sea - Løseth et al. (2022)
Central North Sea - Ottesen et al. (2018)
Southern North Sea - Kuhlman & Wong (2008)
H
L.P.
Middle Pleistocene
Early Pleistocene
Pliocene
Time (ka)

Figure 2

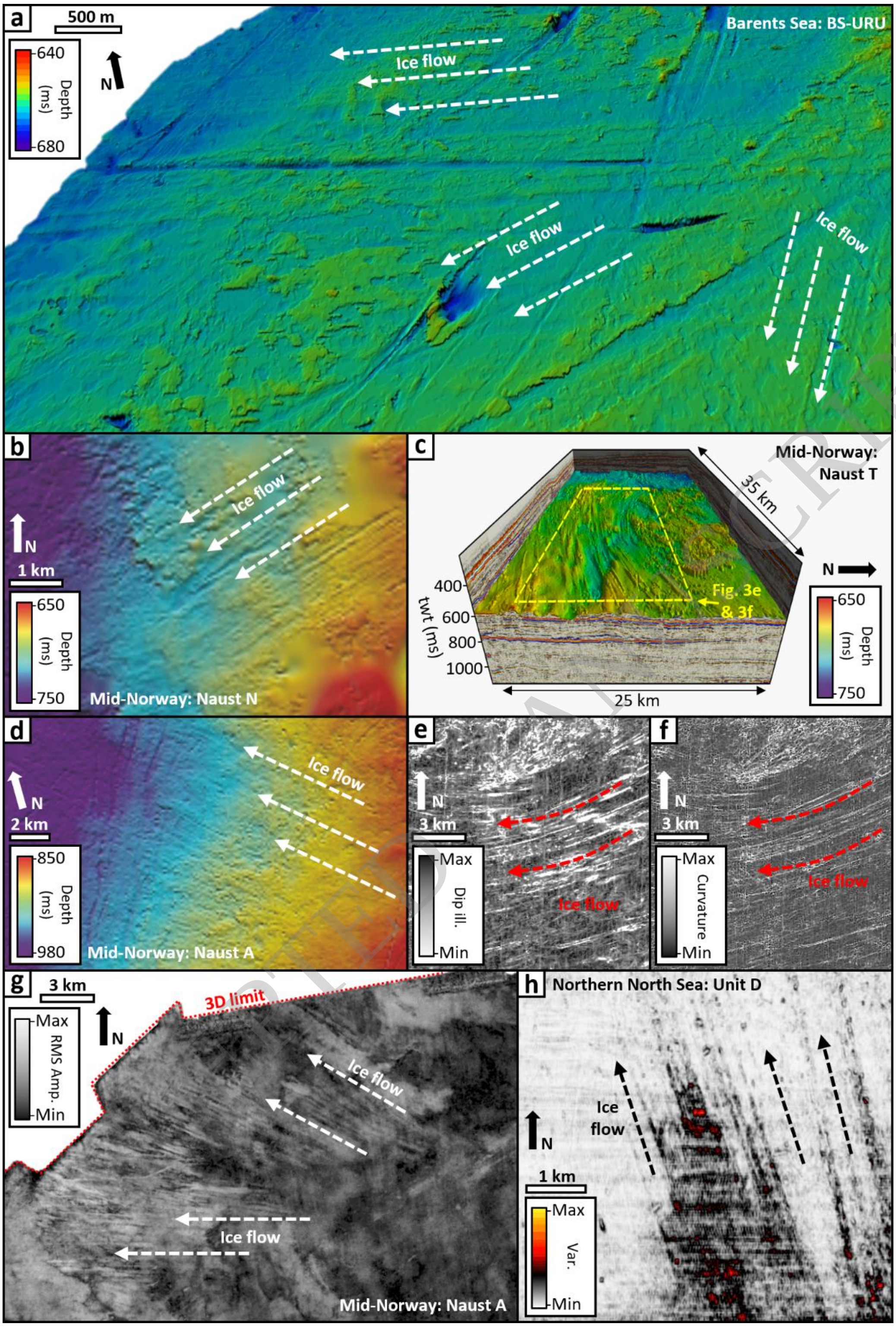
a
500 m
640
680
Depth (ms)
N
Barents Sea: BS-URU
Ice flow
Ice flow
Ice flow
b
N
1 km
650
750
Depth (ms)
Ice flow
Mid-Norway: Naust N
c
Mid-Norway: Naust T
35 km
N
400
600
800
1000
twt (ms)
Fig. 3e & 3f
25 km
650
750
Depth (ms)
d
N
2 km
850
980
Depth (ms)
Ice flow
Mid-Norway: Naust A
e
N
3 km
Max
Min
Dip ill.
Ice flow
f
N
3 km
Max
Min
Curvature
Ice flow
g
3 km
N
3D limit
Max
Min
RMS Amp.
Ice flow
Ice flow
Mid-Norway: Naust A
h
Northern North Sea: Unit D
Ice flow
N
1 km
Max
Min
Var.

Figure 3

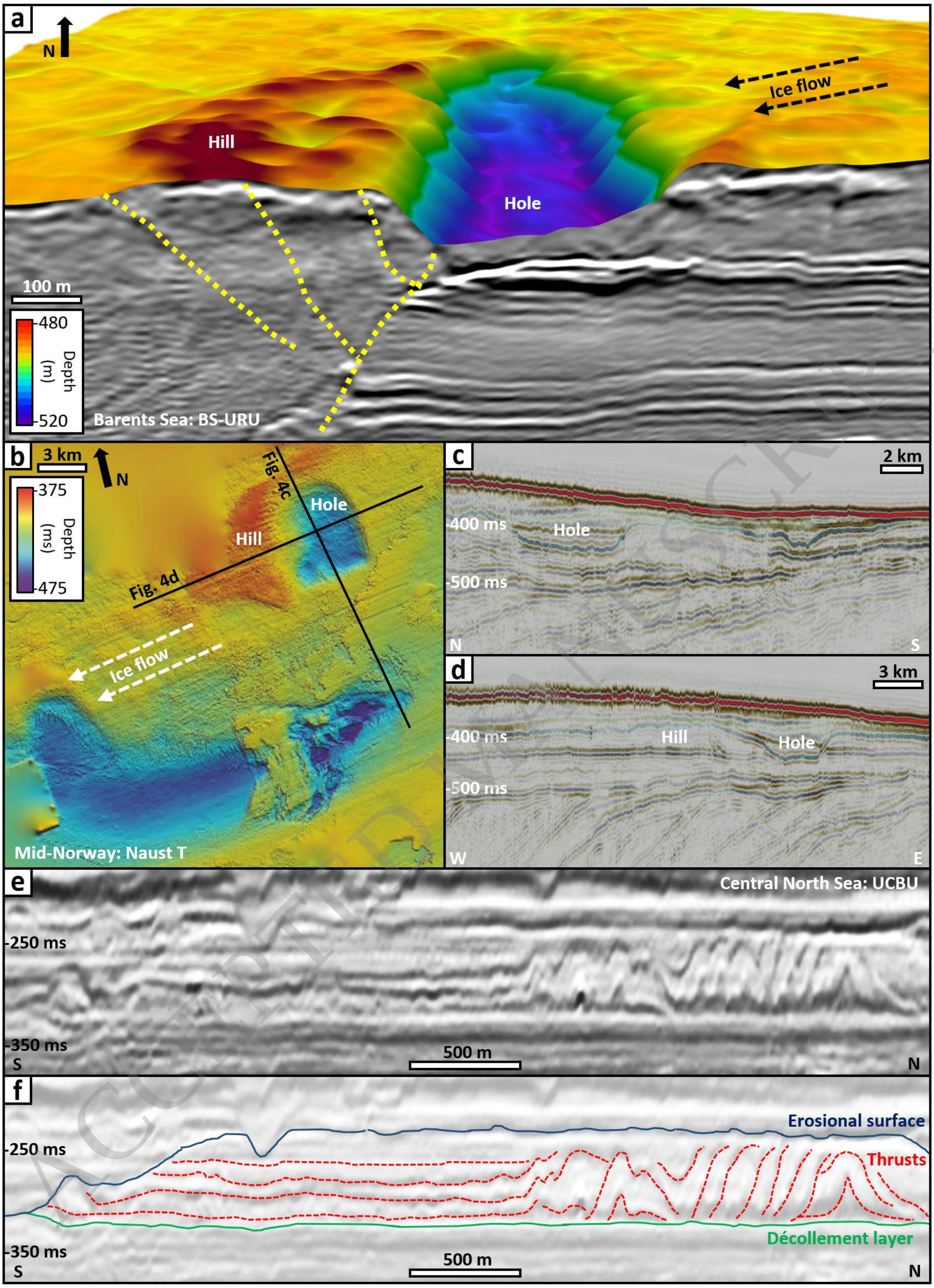
a
N
Ice flow
Hill
Hole
100 m
-480
Depth (m)
-520
Barents Sea: BS-URU
b
3 km
N
Fig. 4c
Hole
Hill
Fig. 4d
-375
Depth (ms)
-475
Ice flow
Mid-Norway: Naust T
c
2 km
-400 ms
Hole
-500 ms
N
S
d
3 km
-400 ms
Hill
Hole
-500 ms
W
E
e
Central North Sea: UCBU
-250 ms
-350 ms
500 m
S
N
f
Erosional surface
-250 ms
Thrusts
Décollement layer
-350 ms
500 m
S
N

Figure 4

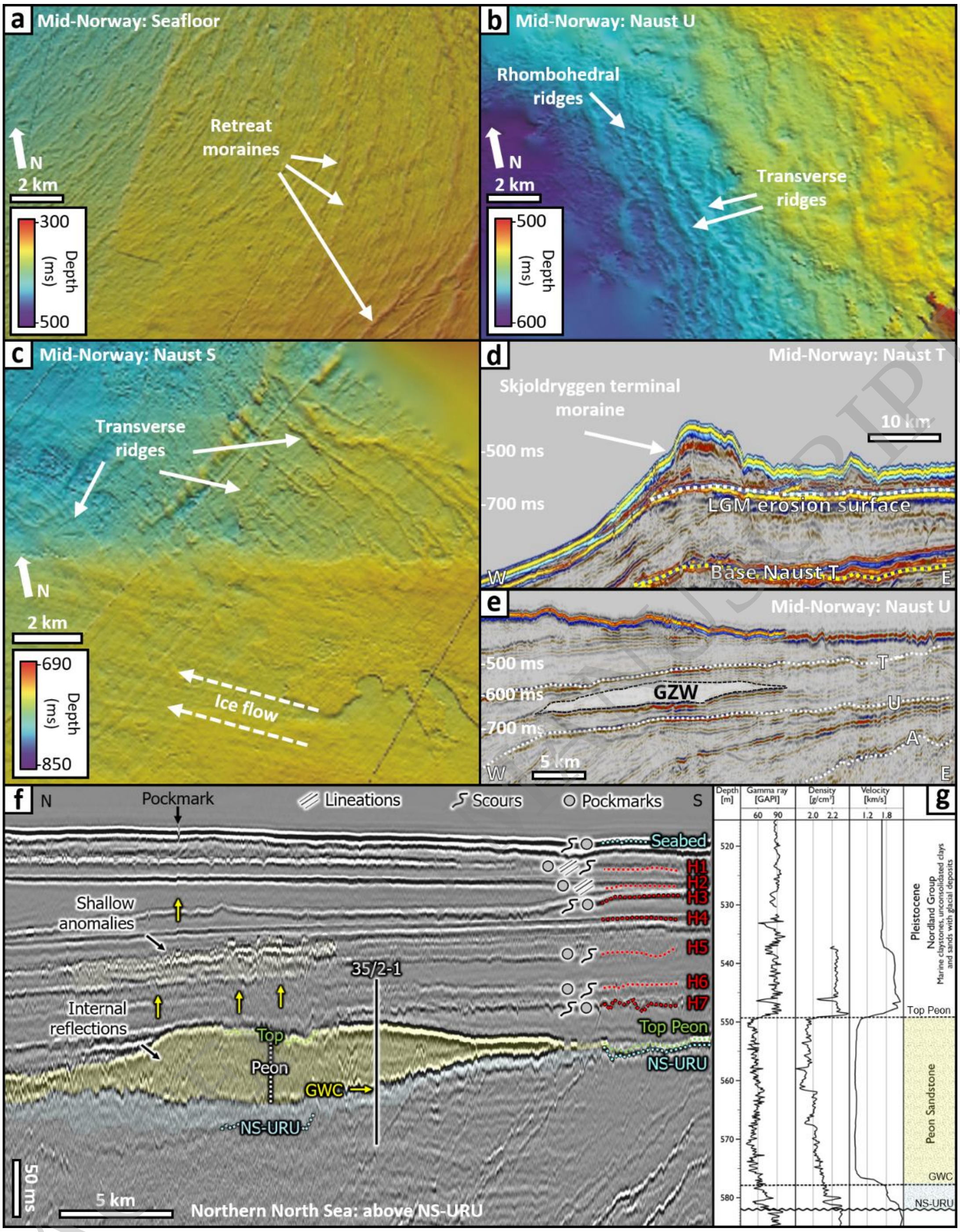
a
Mid-Norway: Seafloor
Retreat moraines
N
2 km
300
Depth (ms)
500
b
Mid-Norway: Naust U
Rhombohedral ridges
N
2 km
Transverse ridges
500
Depth (ms)
600
c
Mid-Norway: Naust S
Transverse ridges
N
2 km
690
Depth (ms)
850
Ice flow
d
Mid-Norway: Naust T
Skjoldryggen terminal moraine
10 km
-500 ms
-700 ms
LGM erosion surface
Base Naust T
W
E
e
Mid-Norway: Naust U
-500 ms
-600 ms
-700 ms
GZW
T
U
A
5 km
W
E
f
N
Pockmark
Lineations
Scours
Pockmarks
S
Seabed
H1
H2
H3
H4
H5
H6
H7
Shallow anomalies
35/2-1
Internal reflections
Top Peon
GWC
NS-URU
50 ms
5 km
Northern North Sea: above NS-URU
g
Depth [m]
Gamma ray [GAPI]
Density [g/cm³]
Velocity [km/s]
Pleistocene
Nordland Group
Marine claystones, unconsolidated clays and sands with glacial deposits
Top Peon
Peon Sandstone
GWC
NS-URU

Figure 5

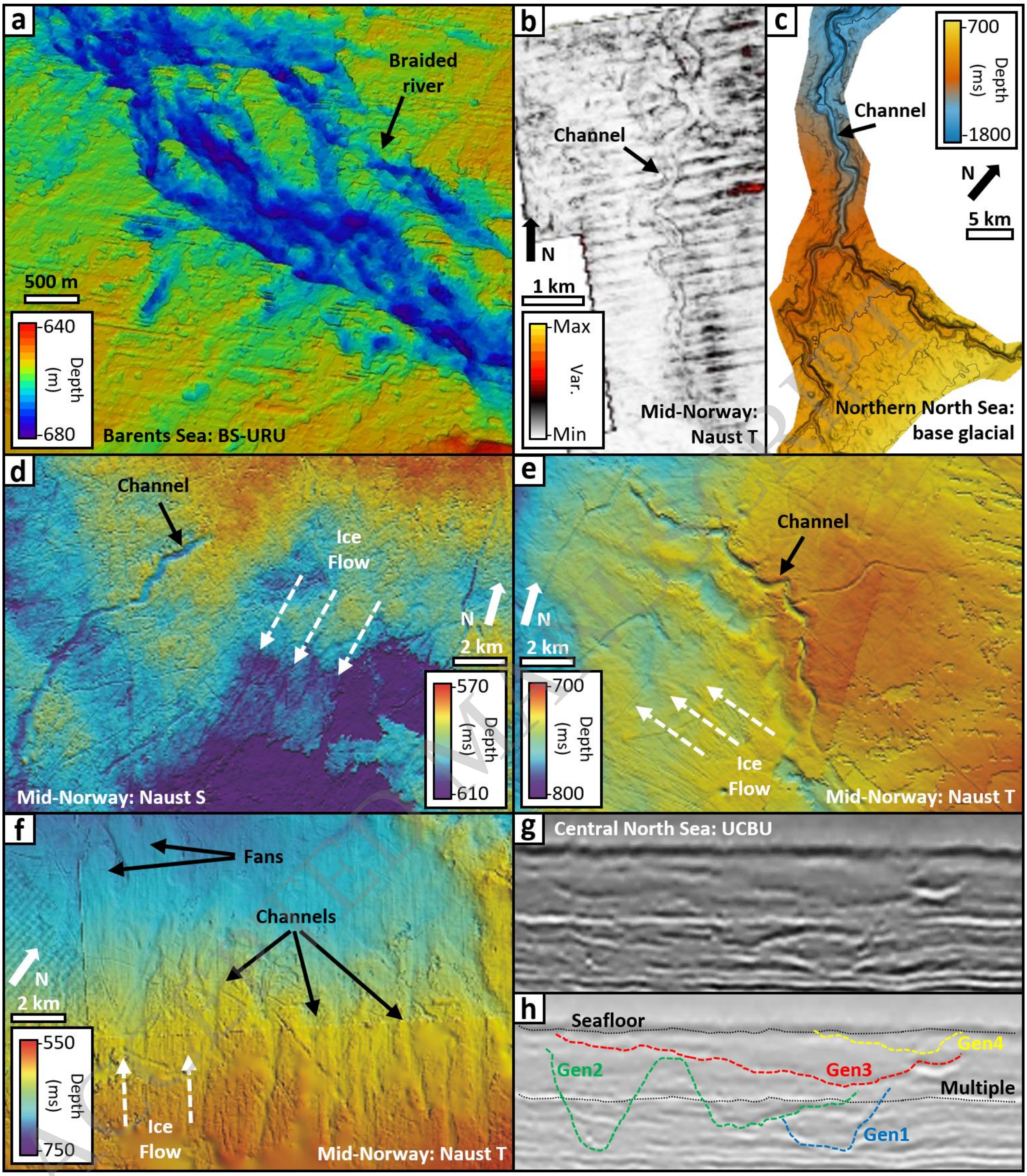
a
Braided river
500 m
640
Depth (m)
680
Barents Sea: BS-URU
b
Channel
N
1 km
Max
Var.
Min
Mid-Norway: Naust T
c
700
Depth (ms)
1800
Channel
N
5 km
Northern North Sea: base glacial
d
Channel
Ice Flow
N
2 km
570
Depth (ms)
610
Mid-Norway: Naust S
e
Channel
N
2 km
700
Depth (ms)
800
Ice Flow
Mid-Norway: Naust T
f
Fans
Channels
N
2 km
550
Depth (ms)
750
Ice Flow
Mid-Norway: Naust T
g
Central North Sea: UCBU
h
Seafloor
Gen4
Gen2
Gen3
Multiple
Gen1

Figure 6

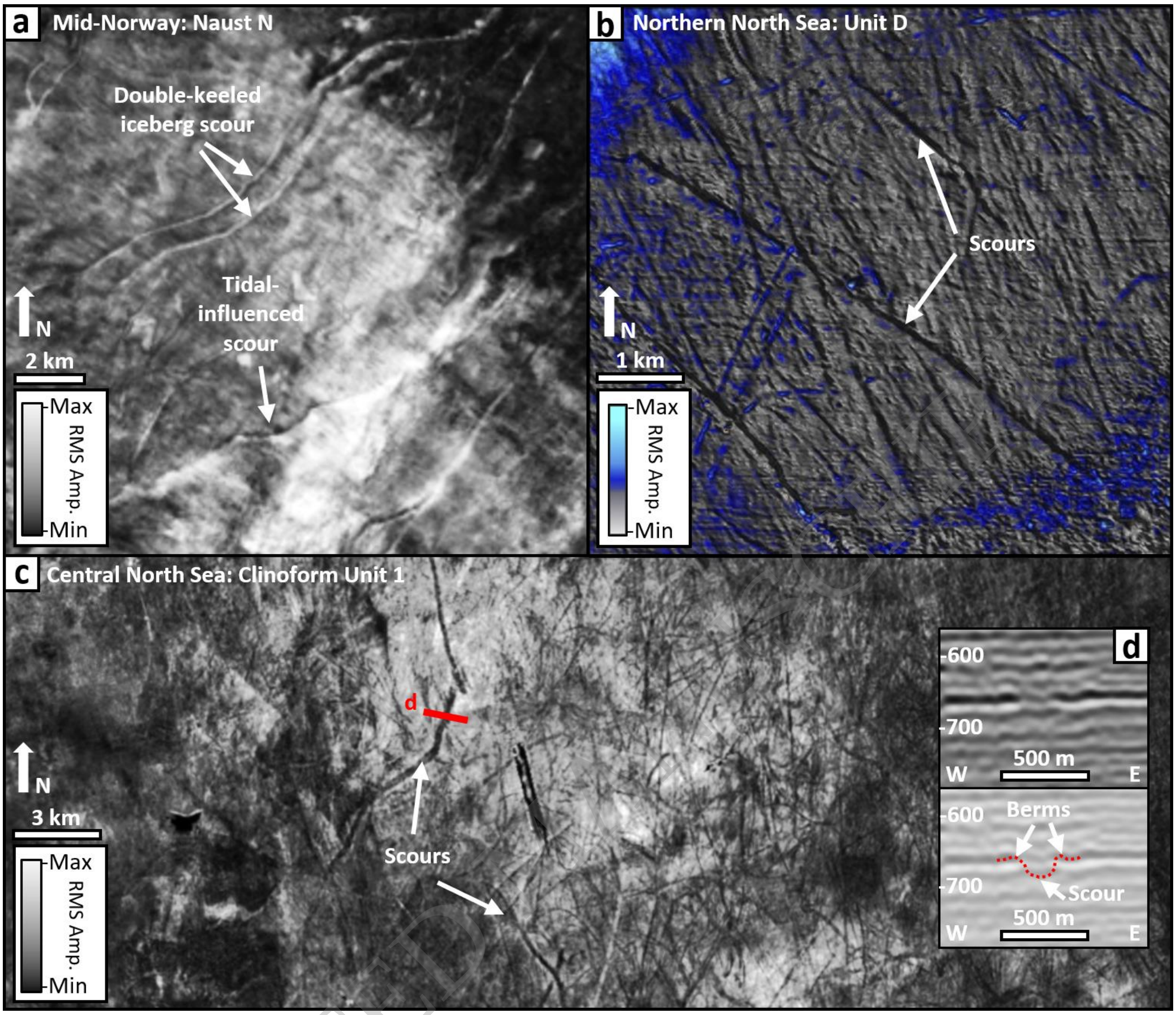
a
Mid-Norway: Naust N
Double-keeled iceberg scour
Tidal-influenced scour
N
2 km
Max
RMS Amp.
Min
b
Northern North Sea: Unit D
Scours
N
1 km
Max
RMS Amp.
Min
c
Central North Sea: Clinoform Unit 1
d
Scours
N
3 km
Max
RMS Amp.
Min
d
-600
-700
500 m
W
E
-600
Berms
-700
Scour
500 m
W
E

Figure 7

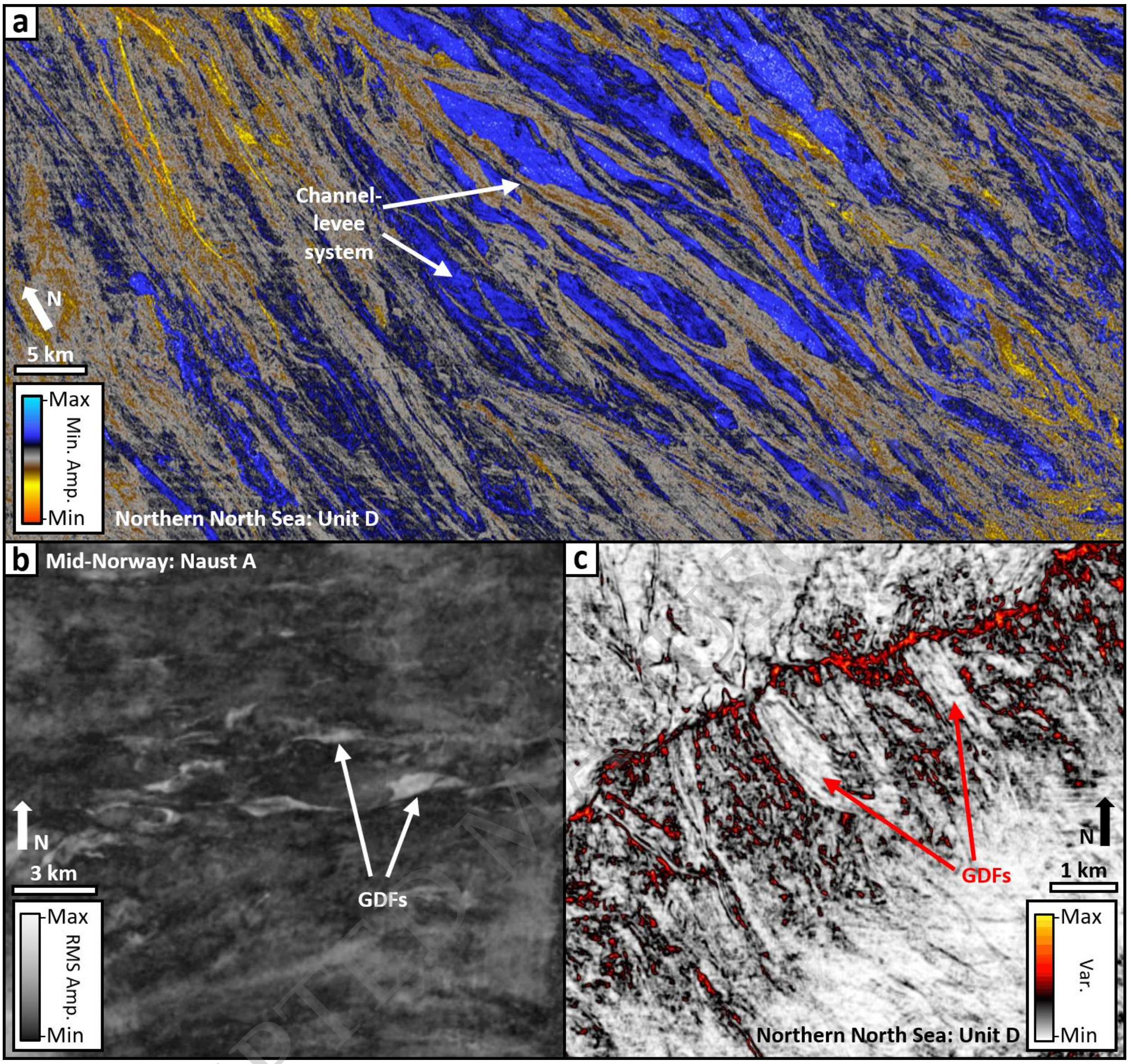
a
Channel-
levee
system
N
5 km
Max
Min. Amp.
Min
Northern North Sea: Unit D
b
Mid-Norway: Naust A
N
3 km
GDFs
Max
RMS Amp.
Min
c
GDFs
N
1 km
Max
Var.
Min
Northern North Sea: Unit D

Figure 8

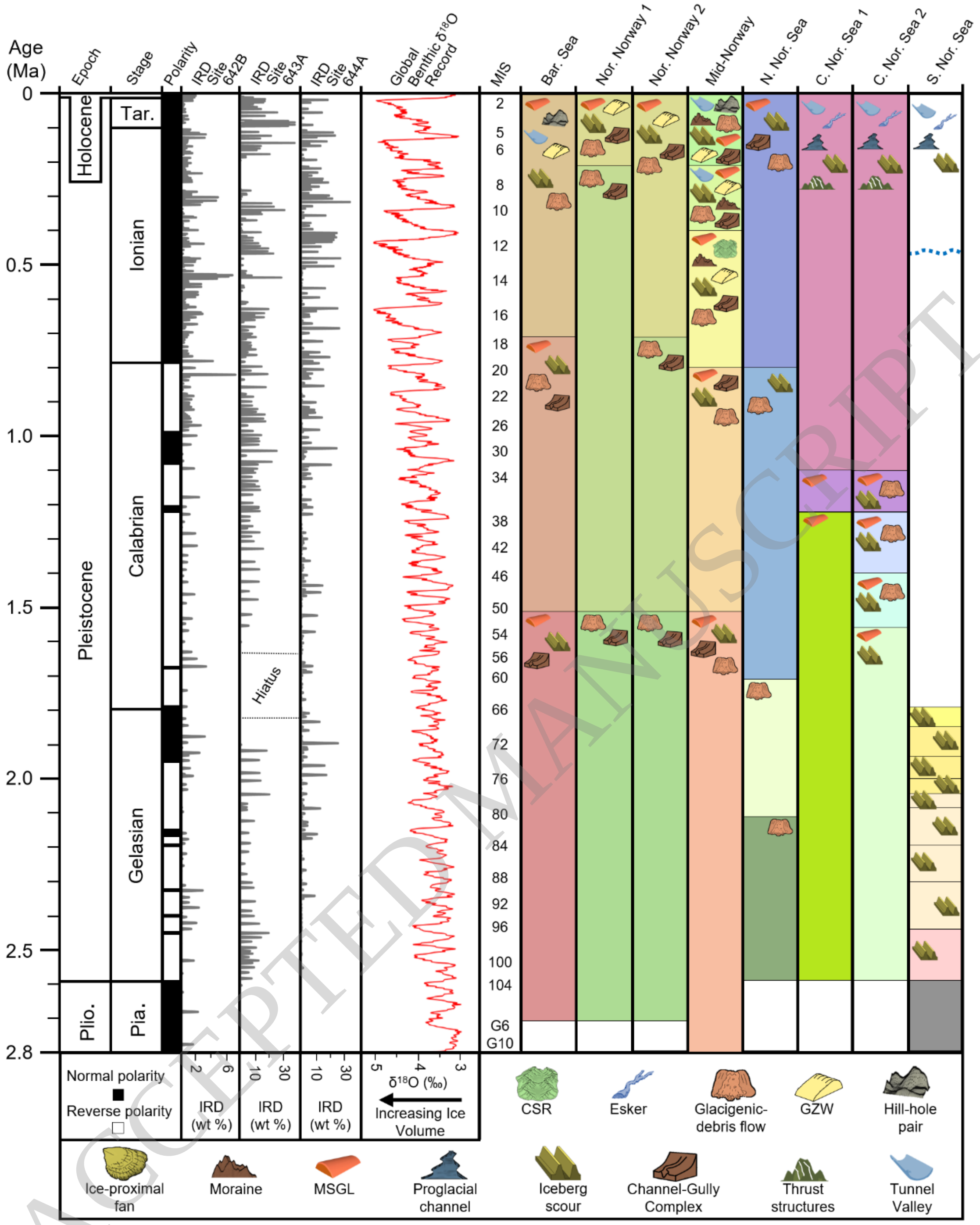

Age (Ma)
Epoch
Stage
Polarity
IRD Site 642B
IRD Site 643A
IRD Site 644A
Global Benthic δ18O Record
MIS
Bar. Sea
Nor. Norway 1
Nor. Norway 2
Mid-Norway
N. Nor. Sea
C. Nor. Sea 1
C. Nor. Sea 2
S. Nor. Sea
Holocene
Pleistocene
Plio.
Tar.
Ionian
Calabrian
Gelasian
Pia.
Hiatus
Normal polarity
Reverse polarity
IRD (wt %)
δ18O (‰)
Increasing Ice Volume
CSR
Esker
Glacigenic-debris flow
GZW
Hill-hole pair
Ice-proximal fan
Moraine
MSGL
Proglacial channel
Iceberg scour
Channel-Gully Complex
Thrust structures
Tunnel Valley

Figure 9